

**I.O.S.**

**PHYSICAL PROCESSES CONCERNING THE MOVEMENT OF  
FLUVIAL GRAVELS AND ITS RELEVANCE TO MARINE  
GRAVELS: A LITERATURE SURVEY**

**F D C HAMMOND**

**REPORT NO 131**

**1982**

**INSTITUTE OF  
OCEANOGRAPHIC  
SCIENCES**

**NATURAL ENVIRONMENT  
RESEARCH COUNCIL**

**INSTITUTE OF OCEANOGRAPHIC SCIENCES**

**Wormley, Godalming,  
Surrey, GU8 5UB.  
(0428 - 79 - 4141)**

**(Director: Dr. A.S. Laughton FRS)**

**Bidston Observatory,  
Birkenhead,  
Merseyside, L43 7RA.  
(051 - 653 - 8633)**

**(Assistant Director: Dr. D.E. Cartwright)**

**Crossway,  
Taunton,  
Somerset, TA1 2DW.  
(0823 - 86211)**

**(Assistant Director: M.J. Tucker)**

---

*On citing this report in a bibliography the reference should be followed by  
the words UNPUBLISHED MANUSCRIPT.*

PHYSICAL PROCESSES CONCERNING THE MOVEMENT OF  
FLUVIAL GRAVELS AND ITS RELEVANCE TO MARINE GRAVELS:  
A LITERATURE SURVEY

F D C HAMMOND

Report No 131

1982

This project was supported financially  
by the Department of the Environment

Institute of Oceanographic Sciences  
Crossway  
Taunton  
Somerset  
TA1 2DW



## CONTENTS

	Page
List of principle SYMBOLS with dimensions	
Mathematical SYMBOLS	
SUMMARY	1
1.0 INTRODUCTION	3
1.1 Defintion of gravel	4
1.2 Relative density of gravel	5
1.3 Particle shape	5
2.0 FACTORS GOVERNING SEDIMENT MOTIONS	6
2.1 Reynold's numbers	7
2.2 Dimensionless drag coefficient	8
2.3 Flow over a rough rigid wall of spheres	10
2.4 Universal resistance law for pipes and open channel flow	11
2.5 Friction factors in tidal channels	13
2.6 The relationship between $k$ , $d$ and $z_0$	14
2.7 Physical interpretations for $z_0$	15
2.8 Experimentally determined velocity profiles	17
3.0 SHIELDS' ENTRAINMENT FUNCTION	19
3.1 The third threshold region of Shields' graph	20
3.2 The fourth threshold region of Shields' graph	21
3.3 Specification of a threshold of sediment motion	23
3.4 Alternatives to Shields' threshold band	23
3.5 Calculated thresholds for different marine gravel sizes	24
4.0 THE INFLUENCE OF NONUNIFORM GRAVELS ON THRESHOLD MOTION	25
4.1 Bimodal sediment distributions	25
5.0 INSTANTANEOUS HYDRODYNAMIC FORCES ON A SOLID PARTICLE	26



CONTENTS (Contd)	Page
6.0 SEDIMENT MOVEMENT THRESHOLD CRITERIA FOR SURFACE WAVES ONLY	29
6.1 Sediment movement threshold criteria for surface waves and currents	30
7.0 THE RELATION BETWEEN BED SHEAR STRESS AND ENGLISH CHANNEL SEDIMENTS	32
7.1 Biota growth on gravel as a measure of gravel stability	32
8.0 SHORE PROTECTION, GRAVEL MOVEMENT AND EXTRACTION	33
9.0 SEDIMENT TRANSPORT FORMULAE	35
9.1 Some considerations of sediment transport formulae	36
10.0 CONCLUSIONS	38

REFERENCES

TABLES

APPENDIX

FIGURES





LIST OF PRINCIPLE SYMBOLS WITH DIMENSIONS

Roman alphabet (upper case)

A	Bed surface plan area	$L^2$
$C_D$	Drag coefficient for a sphere	
$C_z$	Coefficient of friction at the height z above the seabed which, in practice, is usually 100 cm; that is, $C_{100} = (u_* / u_{100})^2$	
D	Internal diameter of a pipe or subscript for a drag force	L
F	The Froude number which is equivalent to $\hat{u} / \sqrt{gh}$	
$F_D$	The drag, or horizontal, force on a sphere	$MLT^{-2}$
L	A length scale	
M	The modulus or measure of the variation of grain size for a unimodal distribution of sand or gravel	
$\hat{M}$	Average moment of tractive forces per unit plan area	$MT^{-2}$
Re	Reynold's number with unspecified length and velocity scales	
$\hat{Re}$	Reynold's number flow scale in terms of mean depth and depth-mean flow velocity	
$Re_\infty^d$	Reynold's number flow scale in terms of a spherical diameter d and relative velocity between fluid and sphere	
$Re_*^d$	Reynold's number flow scale in terms of grain size d and friction velocity $u_*$	
$Re_*^k$	Reynold's number flow scale in terms of rigid wall uniform roughness height k and friction velocity $u_*$	
U	A fluid velocity scale	$LT^{-1}$



Roman alphabet (lower case)

d	Diameter of a sphere or characteristic size for a unimodal sediment grain size distribution	L
$d_{50}$	Median grain size of a unimodal distribution by weight	L
$d_{35}$	The diameter, or abscissa, which partitions the cumulative curve of a unimodal sediment distribution into 35% and 65% of the sample as measured by sieving and weighing	
g	Gravitational acceleration	$LT^{-2}$
h	Mean depth (height) of open channel flow	L
i	Energy gradient or slope of uniform flow	
k	Physical roughness height above datum or equivalent uniform roughness height to an in-situ nonuniform rough surface	
l	Sediment particle saltation distance or hop length	L
n	Number of sediment particles displaced from a bed surface per unit plan area per unit time	
$q_s$	Mobile sediment total load or bed load per unit width per unit time	$ML^{-1}T^{-3}$
$q_{sb}$	Mobile sediment bedload per unit width per unit time	$ML^{-1}T^{-3}$
t	Time interval or period of observation	T
$u_\infty$	The velocity of the stream outside an object's boundary layer; that is, their relative velocity	$LT^{-1}$
$u_z$	The horizontal fluid velocity at height z above the bed which in marine work is usually 100 cm; $u_{100}$ .	
$u_*$	The velocity scale, or friction velocity, near the bed	$LT^{-1}$
$\hat{u}$	The depth-mean velocity at a vertical section of open channel flow	$LT^{-1}$
w	Dry weight of a sediment particle	$MLT^{-2}$
z	The coordinate for height above the bed	L
$z_0$	The zero-velocity height above datum as determined from the von Karman-Prandtl velocity profile	L



Greek alphabet (upper case)

$\Xi$	A dimensionless quantity designed to eliminate $u_*$ from one axis of Shields' graph	
$\Psi$	Einstein's sediment-flow intensity number; equivalent to $\theta^{-1}$	

Greek alphabet (lower case)

$\delta$	The thickness, or height, of the viscous sublayer which is hardly ever more than a few millimetres thick	L
$\eta$	Bed particle packing coefficient; equivalent to the number of surface particles per unit plan area multiplied by the area	
$\epsilon$	A small number that Neil and Yalin suggest should be adopted conventionally to denote the beginning of bed load movement; equivalent to $nd^3/u_*$	
$\theta$	Shield's entrainment number; equivalent to $\rho u_*^2 / g(\rho_s - \rho)d$	
$\theta_c$	The critical value of $\theta$ when bed particles begin to move	
$\kappa$	Von Karman's constant ( $\approx 0.4$ )	
$\lambda$	The friction factor which is proportional to $(u_*/\hat{u})^2$	
$\nu$	The kinematic viscosity of the fluid which is equivalent to $\mu/\rho$ and for sea-water is approximately equal to $0.011 \text{ cm}^2/\text{s}$	$L^2 T^{-1}$
$\rho$	Relative density of fluid	
$\rho_s$	Relative density of sediment particles. A typical value for sand and gravel is 2.65	
$\tau_0$	Mean bed shear stress for a levelled bed and is equivalent to $\rho u_*^2$	$ML^{-1} T^{-2}$
$\tau_\omega$	Maximum bed shear stress on a levelled bed due to surface wind-waves	$ML^{-1} T^{-2}$
$\tau_{\omega 0}$	The bed shear stress due to the combination of $\tau_0$ and $\tau_\omega$	$ML^{-1} T^{-2}$
$\mu$	Dynamic viscosity of the fluid	$ML^{-1} T^{-1}$
$\emptyset$	Dimensionless sediment transport rate	
$\chi$	The elevation above an arbitrary datum at which the mean bed shear stress appears to act	L



MATHEMATICAL SYMBOLS

$\underline{u}$	Vector quantity; eg velocity vector
$D/Dt$	Substantial derivative, or the derivative of a function dependent on time and spatial coordinates
$\nabla^n$	Laplacian operator to the power n; eg $\nabla^2 \underline{u} \equiv \left( \frac{\partial}{\partial x} + \frac{\partial}{\partial y} + \frac{\partial}{\partial z} \right) \underline{u}$
$\equiv$	Equivalent to
$=$	Equal to
$e$	Exponential value ( $\approx 2.72$ )
$f$	Function symbol
$\pi$	Pi constant ( $\approx 3.14$ )
$\approx$	Approximately equal
$< >$	Less, or greater than
$\ll \gg$	Less, or greater than by at least an order of magnitude
$\sim$	An order of magnitude equality
$\propto$	Proportional to
$\leq \geq$	Less or equal to: greater or equal to
$ \underline{u} $	Magnitude of the vector $\underline{u}$





## SUMMARY

It is important to find the causes of long-term and short-term evolutionary changes to the near-shore marine environment. Some of these changes are caused intentionally or inadvertently by industry, local government and other organised or unorganised human activity. The reasons why gravel occurs in a particular location and its subsequent movement is just one aspect of an environment to be explained. Gravel is important to the construction industry and to fisheries. Also, gravel beds are a major natural defence protecting the coastline from excessive erosion. The physics of gravel movement is reviewed here in order that marine scientists and engineers can predict the conditions in which gravel moves naturally.

This report is a review of the literature on the movement of gravel by water. Most of the studies relate to unidirectional flow in rivers. However, it is known from observations using under-water television that quite large gravel can be moved by tidal flow in confined channels such as the West Solent, Isle of Wight, UK. It is normally assumed that tidal flow is unidirectional for sufficiently long periods for the results derived from river analyses to be relevant to the marine environment. This report helps to define conditions where this assumption can be tested by field experiments in the sea.

The extensive literature dealing with the transport of solid particles by fluid streams describes experiments and observations which fall into three main categories:

- i. The determination of the stream conditions just giving rise to the initial solid grain motion; ie the threshold condition.
- ii. The aggregate mass of sediment moved by a given flow in a given time; ie sediment transport rates.
- iii. Studies of the formation, and drag effect on the fluid, of bedforms such as dunes and sandwaves. Very little has been published on the formation of seabed gravel-waves which can be strong side-scan sonar reflectors from the seabed.

From laboratory experiments, the physics of movement of non-cohesive sediments by fluids are well-known in principle but there are many scaling problems when this understanding is applied to the sea. For instance, it is possible in a flume to assess directly by measurement the turbulent fluid forces acting second by second on individual large spheres. However, in the sea, of course, natural conditions are much more complex and in particular, gravel is fairly random in size and angularity. Near-shore oceanographers and marine geologists have to consider much longer-time scales, a century or more, to reveal trends of coastal evolution which may escape detection by applying conventional fluid mechanics. In this situation it is the extreme events that may dominate the transport processes and it is unlikely that measurements are made at these times.

The problems of predicting sediment transport rates are of such a complexity in their detail that even with controlled flume experiments, discrepancies between the results reported by individual experimenters are common-place. The extent of the practical problem of predicting sediment transport rates can be envisaged since more than 80 sediment transport formulae have been published over the past 200 years; some of which require the determination of 4, or more, empirical constants. When the sediment transport rate is well above initial movement, the difference between the lowest and highest prediction is over 2 orders of magnitude. On the seabed, the total mass transport rates of gravel as compared with sand are not likely to be large. Consequently this report concentrates on initial gravel movement. Six extant transport formulae, five of which have been fitted specifically to measured gravel transport rates in rivers and flumes, will be reviewed.

## 1.0 INTRODUCTION

It is well-known that some severe storm-waves can devastate a coastline. There is also a persistent displacement of beach material, including gravel, which occurs under the action of smaller waves. The persistent, but generally small, displacement of gravel can continue further off-shore from the UK coastline where the forces at work are likely to be tidal as well as wind-wave in origin. Pebbles, cobbles and boulders are readily seen to be moved as beach material due to the effects of waves. A problem that needs an answer is whether this material is derived from coast erosion and transported by long-shore drift only, or whether tidal flow and waves are capable of moving at least some of this sediment to the coast from comparatively deep water deposits. It is important that offshore gravel extraction does not stop material reaching the beach. Consequently, it is of economic interest to predict in any area whether gravel will move, when, and how much.

However, there is considerable work to be done in verifying existing ideas concerning the independent effects of waves and currents on sediments. In this respect, almost no work has been carried out in the marine environment to test that gravel, in particular, responds as predicted for the transport of gravel in open channel turbulent flow (ie in the absence of wind-wave orbital motion). Initially, it will be necessary to test that laboratory threshold values for gravel movement are applicable in open sea conditions. To quantify how much bed material is transported and re-worked by waves and tides on, say, an annual time-scale one needs to know precisely what are the forces at work, whence they come and whether they vary from year to year. One way to test the system is to use hydraulic engineering sediment transport formulae and see how well they can predict the transport of loose granular material on the sea bed. Quite clearly we need a formula that can predict the effects of waves and tides on bed material. Such formulae are in the very early stages of development, although some progress has been made by the use of a wave enhancement factor on tidal currents (eg Bijker, 1967). Recently, Swart (1976) has compared 3 unidirectional sediment transport formulae modified by Bijker's enhancement factor for the prediction of sediment transport under the combined action of waves and tides. One conclusion was that the Ackers and White formula (Appendix A) should be chosen as the basis for computation. The increase in the sediment transport rate for a sand fraction due to the maximum enhancement factor is quoted by Heathershaw and

Hammond (1979), and utilised in the Swansea Bay beach erosion study by Wilkinson (1980). Assuming Bijker's physical premises are acceptable, with the aid of the modern computer, it is comparatively straightforward to apply the enhancement factor to existing formulae designed for unidirectional flows.

Bedforms such as gravel-waves (~20 metres long) cannot be scaled properly in the laboratory and it will be necessary to test if form drag can be added linearly to gravel particle drag in accordance with the theory for flow over bedforms in rivers (Yalin, 1977). From studies of flow over rigid wedge-shaped replicas (Engel and Lau, 1980) it is by no means certain that form drag and particle drag (skin friction) can be added linearly. Studies done on wind-wave oscillatory fluid motion over sand ripples (Davies, 1980) and unsteady tidal flow over sand ripples (Dyer, 1980) may provide useful guidelines for similar studies on gravel-waves.

Bedform drag and bed shear stress (skin friction) have an important effect on the distribution of tide and wave energy. For instance, it has been demonstrated by numerical simulation (Wang and Wilson, 1979) that large-scale sand or gravel extraction in the lower bay of New York harbour could change the tidal elevations along Staten Island by up to 12 cm. This is a significant change in tidal elevation, but the different amounts of wave energy incident on a coastline due to gravel extraction (Kinsman et al, 1979) could be even more significant for coastline erosion.

A large part of this report is concerned with reviewing the theoretical and experimental evidence from flumes and rivers for the movement of gravel and the larger size fractions. This information will be of value for comparison with the flow conditions that occur over gravel beds in the sea.

#### 1.1 Definition of gravel

The term gravel is used in geology to define a precise grain size, and is applied to grains larger than coarse sand and smaller than pebbles; ie 2 mm to 4 mm in diameter. The term, however, is also used stratigraphically and by hydraulic engineers in a much looser sense, eg river gravels and glacial gravels containing a mixture of particles which may range from medium sand to boulders.

The widely accepted international geological standard for particle size is the Wentworth-Udden scale (Table 1).

The size range of interest in this report is from gravel to boulder; but generally restricted to gravels and pebbles (2 mm-64 mm). When it is necessary to use the term 'gravel' explicitly as a species in the context of the Wentworth-Udden scale the size range will be appended to avoid ambiguity.

Gravel and pebble grades found on beaches or off-shore bars are usually referred to as shingle. It is possible that shingle is sometimes a lag deposit accumulation of ancient river gravel, once buried but now exposed by waves and tides.

### 1.2 Relative density of gravel

The initial movement of gravel by flowing water depends partly on relative density of the grains. It is generally assumed in the sediment transport literature that gravels, as with sands, have a relative density close to that of quartz sand ( $\text{SiO}_2$ ); that is, 2.65. For English Channel beach deposits this choice of relative density is reasonably accurate since, for instance, 98.9% of the pebbles and cobbles that make up Chesil Beach, Dorset, UK are composed of chert (cryptocrystalline silica) and flint (a variety of chert), both of which have a relative density of 2.60 (Carr and Blackley, 1969).

### 1.3 Particle shape

Since pebble shape may be important for the threshold of particle motion the shape characteristics of pebbles are often quoted in the literature. Let the orthogonal semi-axes be a, b and c in order of decreasing size. The more common indices for shape, as quoted by Carr et al (1974) are:

- i. Wentworth-Cailleux's flatness index  $(a + b)/2c$ ;
- ii. Krumbein's sphericity index  $(bc/a^2)^{1/3}$ .
- iii. Sneed and Folk's maximum projection index  $(c^2/ab)^{1/3}$ .

For a sphere each of the indices will equal unity. As an example, the sphericity index for Chesil Beach quartzite and flint are typically 0.65 and 0.72 respectively, which indicates that the flint pebbles on this beach are generally more spherical than quartzite. Using another sphericity index  $(c/(ab)^{1/2})$ , Dyer (1969) found that

the index for West Solent gravel was 0.46.

Because of their shape, particularly for the flatter grains, gravel particles will tend to slide along the bottom rather than rolling. However, because of fluid acceleration over the upper leading edge of the plate there will be considerable lift which will enhance motion. According to Pettijohn (1975) the hydrodynamically most stable arrangement of densely packed grains is with the long axis pointing downstream. A transverse orientation is observed for loosely packed grains. The nearly flat gravel thus lies like roof tiles. This phenomenon is called imbrication and the transverse orientation has been confirmed experimentally by Sarkisian and Klimora (1955) and Kelling and Williams (1967). As reported by Pettijohn (1975), Cailleux (1945) found from the stratigraphic record that imbrication was common in rocks of fluvial origin but less common in marine sedimentary rocks. The effect of pebble shape and orientation does not appear to have been studied systematically (Neil, 1968a) although the general notion of 'armouring' is often mentioned; for example, Gessler (1971) and Bagnold (1980). The process of armouring described by Taylor and Vanoni (1972) is no more than a lag deposit of larger, denser particles where unburied finer, less dense particles have been eroded away,

Usually, the diameter of a 'sphere' is used to calculate gravel threshold motion. For slaty, or flaky particles, Mantz (1977) used the diameter of a hypothetical sphere equal in volume. It is to be noted that the threshold values observed by Pang (1939) and Schoklitsh (1949) for slates with hypothetical diameters 1.6-6.7 mm are more or less the same values as found by experimenters using truly spherical solid particles (see section 3.0 and Fig 2d).

## 2.0 FACTORS GOVERNING SEDIMENT MOTION

If an alluvial stream has sufficient velocity the solid particles of the bed will begin to move. The various factors that govern the movement will include the grain diameter  $d$ , relative density of grains  $\rho_s$  and water  $\rho$ , the kinematic viscosity of the water  $\nu$  and the shear stress the water exerts on the bed. These variables can be formed into dimensionless groups. The use of dimensional analysis is extremely important in sediment transport problems (Yalin, 1977) since it reduces the number of variables involved. Two important dimensionless

numbers are the Reynolds Number  $Re$  and the dimensionless drag coefficient  $C_D$ .

Before examining the threshold characteristics of sediment particles, it is necessary to review briefly the basic principles of water flow over a sediment bed. Extensive laboratory measurements have established formulae describing the resistance of rough pipes to water flow, but the difficulty involved in applying these to tidal channels is that the surface water slopes cannot be measured to allow calculation of the bed shear stress. The alternative method of calculation from the measured velocity profile close to the bed introduces difficulties relating principally to the level within the surface grains at which the velocity on average is zero.

## 2.1 Reynold's numbers

Fluid near the bed will impart momentum to the solid particles. The rate of change of momentum per unit fluid volume following the fluid is

$$\rho \frac{D\mathbf{u}}{Dt} = \rho \frac{d\mathbf{u}}{dt} + \rho \mathbf{u} \cdot \nabla \mathbf{u} \quad (2.1.1)$$

If the flow is steady and incompressible we have

$$\rho \frac{D\mathbf{u}}{Dt} = \rho \mathbf{u} \cdot \nabla \mathbf{u} = -\nabla p + \mu \nabla^2 \mathbf{u} \quad (2.1.2)$$

Where  $-\nabla p$  is the pressure force term and  $\mu \nabla^2 \mathbf{u}$  is the viscous force term. The term  $\rho \mathbf{u} \cdot \nabla \mathbf{u}$  which has the dimensions of mass times acceleration per unit fluid volume is called the inertial force.

The inertial and viscous terms in equation (2.1.2) have dimensions, or order of magnitude scales:

$$|\mathbf{u} \cdot \nabla \mathbf{u}| \sim U^2/L \quad \text{and} \quad |\nabla^2 \mathbf{u}| \sim U/L^2 \quad (2.1.3)$$

The Reynold's number  $Re$  is defined by

$$Re \equiv \frac{\text{Inertial force}}{\text{Viscous force}} \sim \rho UL/\mu = \frac{UL}{\nu} \quad (2.1.4)$$

For simple flows, geometric similarity of the immersed bodies together with equality of the Reynold's numbers ensures dynamic similarity of the flows. For this reason of all dimensionless groupings the Reynold's number is particularly important. There are several Reynold's number scales but it is debatable whether water flow over a sediment can always be represented adequately by a single length scale.

## 2.2 Dimensionless drag coefficient

The resultant drag force  $F_D$  on a sphere of diameter  $d$  with Reynold's scale  $Re_\infty^d$  (ie with constant velocity  $u_\infty$  relative to a boundless fluid) must be in a direction through the centre of the sphere and opposite to the uniform motion. From symmetry, no force is possible perpendicular to this line of action. In general, for a viscous fluid the resultant force  $F_D$  can only be determined empirically and it has been convenient to define a dimensionless drag coefficient  $C_D$  where

$$C_D = F_D / \frac{\pi}{8} \rho u_\infty^2 d^2 \quad (2.2.1)$$

Fig 1(a) shows the variation of  $C_D$  with  $Re_\infty^d$ .

For  $Re_\infty^d$  less than unity:

$$C_D \propto 1/Re_\infty^d \quad \text{and} \quad F_D \propto u_\infty d \quad (2.2.2)$$

called the linear friction law. Equation (2.1.2) reduces to



$$\mu \nabla^2 \underline{u} = -\nabla p \quad (2.2.3)$$

which has been solved analytically and is well-known as Stoke's Law for a sphere in a creeping viscous fluid (Tritton, 1977).

For  $10^3 < Re_{\infty}^d < 10^5$

$$C_D \approx \text{constant and } F_D \propto u_{\infty}^2 d^2 \quad (2.2.4)$$

which is the quadratic friction law. Equation 2.1.2 reduces to Euler's equation

$$\rho \underline{u} \nabla \underline{u} + \nabla p = 0 \quad (2.2.5)$$

The functional relation  $C_D = f(Re_{\infty}^d)$  in Fig 1(a) can be determined by measuring the free fall terminal velocity of a sphere in a 'boundless' stationary fluid. The relation is important for an appreciation of threshold solid particle motion relative to an alluvial stream bed.

Coleman (1972) has produced experimental evidence indicating that, for Reynolds numbers  $R_{\infty}^d$  from about 70 to  $10^5$  the drag coefficient function for a stationary sphere resting on a bed of closely packed identical spheres (Fig 1b) resembles that for a sphere falling with terminal velocity in an infinite fluid (Fig 1a). The experimental points are calculated using the average of one minute readings of a flow velocity, presumably sufficiently far upstream so that  $\partial u_{\infty} / \partial x = 0$ , in a line parallel with a bed through the test sphere's centre. The measured drag force  $F_D$  is also directed along this line. Thus, apart from the scatter of the experimental points, the wall boundary layer has little effect on the drag coefficient (cp Fig 1a-b). The velocity  $u_{\infty}$  is usually defined as the 'free' velocity outside a boundary layer. Coleman's results suggests that a more important definition here is that  $u_{\infty} = |\underline{u}|$  where  $\partial u_{\infty} / \partial x = 0$  and  $\underline{u}$ , the horizontal mean velocity component, intersects the test sphere's centre.

### 2.3 Flow over a rough rigid wall of spheres

If a number of spheres form a horizontal, almost impervious, rough rigid wall then the Reynold's scale appropriate to the boundary layer is the wall roughness number

$$Re_*^k = u_* k / \nu = k \sqrt{\tau_0 / \rho} / \nu \quad (2.3.1)$$

where  $u_*$  is the friction velocity which is the appropriate velocity scale for flow close to the wall.  $u_* = \sqrt{\tau_0 / \rho}$  where  $\tau_0$  is the bed shear stress. If the boundary layer is turbulent a thin viscous film may be attached to the boundary and substantial fraction of the total mean velocity change occurs within this viscous layer. The viscous sub-layer velocity profile is linear:

$$u_z / u_* = zu_* / \nu \quad (2.3.2)$$

Where the thickness  $\delta$  of the viscous sub-layer is given approximately by  $11.0\nu/u_*$  (Tritton, 1977; Yalin, 1977).

Caldwell and Chriss (1979) have a measured viscous sub-layer 6 mm thick on a bed of smooth silty mud in a sea 200 metres deep. Small particles will be embedded totally within the viscous sub-layer, but when the sediment diameter becomes a significant fraction of the sub-layer thickness, the viscous sub-layer is likely to mould itself to the 'roughness' elements so the position of an absolute datum for rough level fluvial beds is difficult to define (see Table 2). It will be assumed here, following the work of Nikuradse and Shields (Yalin, 1977) that an absolute viscous sub-layer of uniform thickness  $\delta$  can exist and it has a common datum with the roughness elements of height  $k$ . The existence of the viscous sub-layer will prove to be important for the gravel threshold condition.

## 2.4 Universal resistance law for pipes and open-channel flow

For open-channel (river) flow of mean depth  $h$  and large width over a flat uniform rigid carpet of solid spheres, each with roughness height  $k$ , the velocity or flow resistance law, is

$$\frac{u_z}{u_*} = \frac{1}{\kappa} \ln\left(\frac{z}{k}\right) + B = f(\text{Re}_*^k) = f\left(\frac{k}{\delta}\right) \quad (2.4.1)$$

and  $\lambda^{-1} \propto \hat{u}^2/u_*^2$  is the friction factor (Yalin, 1977). (2.4.2)

where  $\hat{u}$  is the depth mean flow velocity.

For all practical purposes the boundary layer with the exception of the viscous sublayer (where it exists) is turbulent and occupies the full flow thickness  $h$ . Fully turbulent open-channel flow is defined by the flow Reynold's number.

$$\hat{Re} = \hat{u}h/\nu > 2000 \quad (2.4.3)$$

The existence, or apparent absence, of a viscous sublayer leads to two sub-definitions of fully turbulent open-channel flow: that is,

Hydraulically Smooth Flow  $\hat{Re} > 2000$ ,  $\text{Re}_*^k < 5$ ,  $k < \delta$  (2.4.4)

and

Hydraulically Rough Flow  $\hat{Re} > 2000$ ,  $\text{Re}_*^k > 70$ ,  $k > \delta$  (2.4.5)

The values  $\text{Re}_*^k = 5$  and  $\text{Re}_*^k = 70$  are based on successful pioneering studies such as Prandtl's boundary layer theory and Nikuradse's (1933) experiments of flow impedance in pipes of diameter  $D$  with interior uniform sand roughness  $k$ , but are

not fully substantiated for open-channel flows. Nikuradse determined that for pipes

$$\lambda^{-1} \propto Re = \frac{\hat{u}D}{\nu} \text{ when } Re < 2000$$

and

(2.4.6)

$$\lambda = \text{constant when } Re > 4000$$

However,  $\lambda$  is dependent upon  $D/k$  when  $Re > 4000$  which is not surprising since large changes of  $D/k$  represent a change in pipe geometry rather than a change in pipe roughness. Indeed, the relations 2.4.6 holds only for  $D/k > 15$ .

Colebrook and White (1937) unified Nikuradse's results successfully by introducing a universal semi-empirical resistance law for pipes of non-uniform roughness (eg smooth pipes with rough cement joints) which were determined empirically to be equivalent to Nikuradse's pipes of artificial uniform sand roughness  $k$ ; that is

$$\lambda^{-1/2} = -2 \log_{10} \left( \frac{k}{3.7D} + \frac{2.51\nu}{D\hat{u}\sqrt{\lambda}} \right) \quad (2.4.7)$$

An essential feature of expression 2.4.7 is that at low values of  $Re = \hat{u}D/\nu$  the second term in the brackets predominates and the smooth law is approached, while at high values of  $Re$  the first term predominates and the rough law is approached. When the expression is plotted as a function of  $Re_*^k$  the transition to the smooth law occurs  $Re_*^k = 0.3$ , while the transition to the rough law occurs at  $Re_*^k = 60$  (Webber, 1971).

Assuming a simple geometric equivalence between pipe and channel flow a comparable law, similar to equation 2.4.7, for open-channel flow of non-uniform roughness is

$$\lambda^{-1/2} = -2 \log_{10} \left( \frac{k}{14.8h} + \frac{0.627\nu}{h\bar{u}\sqrt{\lambda}} \right) \quad (2.4.8)$$

Formula (2.4.8) has not been universally adopted because the boundaries and flow characteristics are so variable. However, the method of its derivation (Webber, 1971) does permit an estimate that turbulent flow begins approximately at  $\hat{R}e = 2000$ . It has been established (Grass, 1971) that the transitional zone  $3 < Re_*^k < 70$  is the appropriate range between hydraulically smooth and hydraulically rough flow in a laboratory flume.

## 2.5 Friction factors in tidal channels

An attempt has been made to extend the successful formulation of the resistance law for pipes to tidal channels (Sternberg, 1968). This entails use of a bed shear stress determined from the velocity profile close to the bed rather than from water surface slopes.

The velocity profile close to the bed has been shown (eg Channon and Hamilton, 1971) to conform to

$$\frac{u_z}{u_*} = \frac{1}{\kappa} \ln \left( \frac{z}{z_0} \right) \quad (2.5.1)$$

which implies  $u_z = 0$  at  $z = z_0$ . This is known as the Von Karman-Prandtl equation and is derived on the assumption that in the layer close to the bed the shear stress is constant and the turbulent exchange of momentum is a function of the height above the bed. An alternative, but equivalent, expression to relation (2.5.1) is the drag coefficient  $C_{100}$  defined by

$$C_{100} = u_*^2 / u_{100}^2 \quad (\text{ie } 100 \text{ cm above bottom}) \quad (2.5.2)$$

Comparing (2.5.1) and (2.5.2)

$$C_z = \left(\frac{1}{\kappa} \ln(z/z_0)\right)^{-2} \quad (2.5.3)$$

There is evidently some resemblance between  $C_z$  and the friction factor  $\lambda$ ; ie equations (2.4.2) and (2.5.2).

A relation is easily established since

$$(h-z_0)\hat{u} \approx h\hat{u} = \int_{z_0}^h u dz \text{ for } z_0 \ll h$$

So assuming (2.5.1) is valid for  $z_0 < z < h$

$$\lambda^{-1/2} \propto \frac{\hat{u}}{u_*} = \frac{1}{\kappa} \ln\left(\frac{h}{ez_0}\right) \quad (2.5.4)$$

In a flume, at least, Shields (1936) has established that  $\lambda$  is larger for angular bed sand grains and smaller for rounded sand grains. Shields' experiments also show that  $\lambda$  does not become independent of large  $Re_*^k$  quite so convincingly as it does in pipe flow.

## 2.6 The relationship between $k$ , $d$ and $z_0$

From 2.4.1 and 2.5.1 and as  $\kappa = 0.4$  (Soulsby and Dyer, 1981) we have (Yalin, 1977)

$$\frac{u}{u_*} z = 2.5 \ln\left(\frac{z}{z_0}\right) = 2.5 \ln\left(\frac{z}{k}\right) + B \quad (2.6.1)$$

where  $B = 2.5 \ln\left(\frac{u_* k}{\nu}\right) + 5.5$  when  $Re_*^k < 5$

and  $B = 8.5$  when  $Re_*^k > 70$ .

If  $Re_*^k > 70$

$$2.5 \ln\left(\frac{z}{z_0}\right) = 2.5 \ln\left(\frac{z}{k}\right) + 8.5$$

$$z_0 = k/30 \approx d/30 \tag{2.6.2}$$

This result is reasonable since we would expect for hydraulically rough flow a velocity  $U_d \gg 0$  between the tops of the grains where  $z = d$ . Relations between  $k$ ,  $d$  and  $z_0$  are given in Table 2.

For the hydraulically smooth conditions from (2.6.1)

$$2.5 \ln\left(\frac{z}{z_0}\right) = 2.5 \ln\left(\frac{z}{k}\right) + 2.5 \ln\left(\frac{u_* k}{\nu}\right) + 5.5 = 2.5 \ln\left(\frac{9zu_*}{\nu}\right)$$

$$\text{Hence } z_0 = \nu/9u_* = 0.001/u_*$$

Thus, if  $u_* = 0.42$  cm/s as calculated from measurements made within a viscous sublayer in the marine environment (Caldwell and Chriss, 1970) then  $z_0 = 0.0029$  cm.

By fitting the velocity measurements above the sublayer to the logarithmic form (2.5.1) Caldwell and Chriss obtain the small value 0.00055 cm for the zero-velocity surface height  $z_0$ . At the start of the transitional regime  $Re_*^k \approx 5$ , Yalin (1977) shows that  $\delta \approx 2k$ .

## 2.7 Physical interpretations for $z_0$

A level portion of the seabed does not, of course, consist of identical particles  $k = d$ . There is, however, a uniformly rough surface equivalent to the in-situ surface with some characteristic length  $k$  as shown in Table 2. As mentioned previously, Colebrook and White (1937) were able to find equivalent surfaces even

for roughness elements which were not contiguous. Although river sand and gravel particles are not of uniform size, they are, in general, contiguous. The length  $z_0$  is a function of the shape and density of the elements per unit plan area.

Equation 2.5.1 is the form of the logarithmic profile generally used by oceanographers and meteorologists. The parameter  $z_0$  is often called the roughness height or roughness length scale since, in general, for a level rough bed,  $0 < z_0 < k$  and  $z_0 \propto k$  (Table 2). Using a formula similar to 2.5.4 but with  $k$  instead of  $z_0$  Charlton (1977) finds that if  $h \gg d$ .

$$k = 1.28 d_{50}^{0.82} \quad (0.3 \text{ cm} < d_{50} < 30 \text{ cm}) \quad (2.7.1)$$

with a correlation coefficient of 0.72 where 50%, by weight, of each bed sample was smaller than  $d_{50}$ . For very shallow streams ( $h \approx d$ ) the function (2.7.1) has different numerical values and the correlation is slightly worse.

Without a physical datum it becomes difficult to define  $z_0$  as the zero velocity surface height or effective no-slip boundary displacement. The datum is known in the case of test facilities such as pipes and flumes but it is often not known precisely in oceanography and meteorology. There is some indication of this for Chepil's datum in Table 2 since the mean level of the interface between air and gravel, unlike the other examples, is not a physical datum.

According to Jackson (1981) the logarithmic boundary layer law should be of the form

$$\frac{u_z}{u_*} = \frac{1}{\kappa} \ln \left( \frac{z - \chi}{z_0} \right) \quad (2.7.2)$$

where the displacement height  $\chi$ , as seen by the wall layer flow, is the level where the mean drag  $\tau_0$  appears to act. The wall layer starts at a height  $z > k$  and the mean fluid motion within the wall layer is not deflected by bed roughness. If the average moment of the tractive forces per unit plan area is



$\hat{M}$  then  $\chi\tau_0 = \hat{M}$  where  $\chi$  is the distance  $\hat{M}/\tau_0$  above an arbitrary origin for the vertical co-ordinate  $z$ . Thus, initially, it is unnecessary to define a physical datum as in Table 2. The appropriate velocity scale and apparent origin for the wall layer are  $u_*$  and  $\chi$ . However, for measurements in the sea the errors in the velocity measurements mean that it is difficult to obtain a precise measure of  $\chi$  without long time averages. It is advantageous to use equation (2.5.1) rather than (2.7.2) since the former equation is very much the easier to use in regression analysis. According to Jackson, for uniform contiguous roughness elements, such as all but two of those in Table 2,  $\chi/k \approx 0.7$ ; which implies that the mean bed shear stress appears to act at a height  $0.7k$  above the quoted data.

## 2.8 Experimentally determined velocity profiles

In the sea we are entirely dependent on the accuracy of velocity profile, or turbulence, measurements for the determination of  $\tau_0$ , or equivalently  $u_*$ . From the proceeding discussion it is seen that  $u_*$  is difficult to determine and particularly so if the flow is transitional; that is  $5 < Re_*^k < 70$ . Furthermore, if the flow is unsteady, strongly nonuniform (ie bedforms are present) or carries suspended sediments the actual velocity profiles may depart significantly from the logarithmic profile of equation (2.5.1). The effects of unsteady flow on the interpreted logarithmic profiles have been analysed by Soulsby and Dyer (1981). They calculated that for a realistic tidal situation  $z_0$  would be underestimated by 60% one hour after slack water. The value of  $z_0$  would be overestimated by 83% one hour before slack water. The value of  $u_*$  would be underestimated and overestimated by 20% respectively, and  $\kappa$  would appear to have values of 0.50 and 0.33.

The extent of errors in logarithmic profiles caused by sampling a continuously fluctuating turbulent process has been assessed by Heathershaw and Simpson (1978). They find that typically the bed shear stress is likely to have errors of  $\pm 50\%$  for velocities averaged over 10 minutes. From turbulence measurements Soulsby (1980) has shown that  $z_0$  cannot be estimated to better than about  $\pm 28\%$  with a record length of 10 minutes due to random errors.

Consequently neither the bed roughness length nor the bed shear stress can be defined accurately from velocity profiles. Nevertheless these are values that have to be used.

The presence of bedforms causes a non-uniform flow distribution, with acceleration of the flow over the upstream (stoss) face and a deceleration over the downstream (lee) slope. These effects cause form drag which is additional to the skin friction. Flow separation can occur in the lee of the bedform. Measurements over sand waves have shown that the shear stress at the crest can be four times that in the trough. Bedforms, as roughness elements, have been studied by Smith and McLean (1977), and they provide a method of calculating the drag caused by a hierarchy of superimposed bedforms.

An important observation (Raudkivi, 1976) is the entrainment and bedload transport takes place on bedforms at values of temporal mean bed shear stress well below the threshold shear stress which is reached at more than half-way up the upstream slope. Raudkivi suggests that this phenomenon is due to turbulent agitation. The influence of dune and flow parameters on the friction factor  $\lambda$ , with special reference to the distribution of pressure, has been studied numerically by Sundermann et al (1978) and compared with Raudkivi's experimental results for ripple-size rigid replicas. The model shows excellent agreement with Yalin's (1964) formula for bedform drag. Pressure losses due to skin friction are slightly less than that given by Yalin's formula. The ratio of losses due to skin friction as a percentage of bedform drag losses determined by the model is 14% as compared with Smith's (1977) value of 33% for separating flow over large river sand-dunes.

At the moment there has not been a complete investigation of the variation in the ratio of skin friction to total drag with slope for sedimentary bedforms. However comparison with engineering studies (Knight and MacDonald, 1979) suggests that there is a maximum drag at a steepness value of about  $1/10$ . This is a common value for ripples and megaripples in the sea. Dyer (1980) has postulated that the changes of ripple shape during a tidal cycle may account for a two order of magnitude change in the measured  $z_0$ , because of the variation in the proportion of form drag.

### 3.0 SHIELDS' ENTRAINMENT FUNCTION

It has been known for a considerable time that the detachment of a sediment particle is related to particle weight. Shields' classic (1936) paper used the dimensionless entrainment number  $\theta$ , which is roughly the ratio of the bed mean tractive force divided by the immersed weight of the sediment particle; that is

$$\theta = \frac{\tau_0 d^2}{g(\rho_s - \rho)d^3} = \frac{\rho u_*^2}{g(\rho_s - \rho)d} \quad (3.0.1)$$

This number is particularly useful in river hydraulics since the mean shear velocity near the bed of a wide stream is given by

$$u_*^2 = ghi \quad (3.0.2)$$

where  $i$  is the energy gradient and  $\theta$  is readily calculated. The water surface slope and  $i$  are identical if the flow is uniform and steady.

Shields shows theoretically, and demonstrates experimentally, that

$$\theta_c = f(\text{Re}_*^d) = f\left(\frac{u_* d}{\nu}\right) = f\left(\frac{d}{\delta}\right) \quad (3.0.3)$$

where  $\theta_c$  is the threshold, or critical value of  $\theta$  for detachment of particles from a level bed. It is not surprising that  $\theta_c$  is a function of the grain size Reynold's number  $\text{Re}_*^d$  since just prior to detachment, the flow scales near the bed are characterised by the Reynold's roughness number  $\text{Re}_*^k$  and if the bed is uniformly level  $k \approx d$ . Shields' identified four portions of  $\theta_c$  in terms of  $\text{Re}_*^d$ : Region I ( $\text{Re}_*^d < 2$ ), Region II ( $2 < \text{Re}_*^d < 10$ ), Region III ( $10 < \text{Re}_*^d < 1000$ ) and Region IV ( $1000 < \text{Re}_*^d$ ) as shown in Figure 2. Here, we are particularly interested in the third and fourth regions because of the large value of  $d$  for gravel. In Region 1,  $\theta_c$  is independent of  $d$  (Yalin, 1977). In Region 2,  $\theta_c$  has its most effective value since  $\theta_c$  tends to a minimum near  $\text{Re}_*^d = 10$ . Regions I and II are characterised by the fact that viscous forces, within a viscous sublayer, and

relative density of the solid particles tend to dominate the threshold condition. In Regions III and IV the viscous sublayer becomes much thinner relative to grain size  $d$  (ie  $\delta/d$  tends to zero) and turbulent, or fluctuating, pressure forces dominate the threshold criterion.

### 3.1 The third threshold region of Shields' graph

Shields explains the relation ( $\theta_c \propto Re_*^d$ ) as follow. Although a fixed solid particle in the main flow ( $Re > 2000$ ) would be subjected to quadratic resistance (cp equation 2.2.4), the resistance of 'gravel' in the bed is far from quadratic because the velocity scale  $u_*$  near the bed is much less than  $\hat{u}$ . Shields assumes implicitly that  $Re_\infty^d$  is equivalent to  $Re_*^d$ . This assumption appears to be supported by Coleman's results as plotted in Figure 1b. The drag coefficient  $C_D$  for a 'gravel' bed particle does not lie within the region of quadratic resistance (cp Figure 1a); ie  $C_D$  is not constant. Shields' discussion results in the following simplified expression for the third region.

$$\theta_c \propto Re_*^d \propto 1/C_D \quad (3.1.1)$$

which compared with equation (2.2.2) indicates that the viscous sublayer is still sufficiently thick for the gravel threshold condition to respond as if the flow is laminar. A decrease of  $C_D$  signals an increase in both  $\theta_c$  and  $Re_*^d$  which is in accord with Shields' experimental results. Equation (3.1.1) implies a linear response of the drag force with the local velocity scale; ie  $F_D \propto u_*$  (cp equation 2.2.2 and Figure 1a).

From Grass's (1971) measurements of flow over 9 mm pebbles ( $Re_*^d = 84.7$ ) a poorly developed viscous sublayer is still present in the mean velocity profile. A viscous sublayer is far from being a simple structure and contains unsteady vortex elements. Fluid is transferred to and from the vicinity of the bed in an irregular and intermittent manner. It is not surprising therefore that the instantaneous force distribution on a particle is highly variable for Shields' third region as we would suspect for the fourth region also. It could be that the viscous sublayer is thick only on individual particles for Shields'

third region. However, this does not detract from Shields' argument in anyway.

Later investigators, notably Mantz (1977) and Neil (1968a) have argued that the positive slope of Shields' function is spurious; that is, the function should be as shown in Figure 2(d). Yalin and Karahan (1979) and Taylor and Vanoni (1972) argue equally strongly that the positive slope, as shown in Figure 2(b) and 2(e), is real. Indeed, Taylor and Vanoni say that the function should rise more sharply from the dip than Shields' version. Significantly, Shields suggested that the threshold condition is statistical and would have objected, presumably, to showing the threshold (Figure 2f) as a single (Rouse) curve. It is clear that although Shields' threshold function may be disputed as to details, very little of real consequence has been added or amended at larger grain Reynold's numbers. For a log-log graph the scatter of the experimental points is large.

### 3.2 The fourth threshold region of Shields' graph

Shields explains the significance of the fourth region by analogy with Figure 1a. Again, he assumes that  $Re_*^d$  is equivalent to  $Re_\infty^d$ . The drag force on 'gravel' particles follows the quadratic resistance law; ie  $F_D \propto u_*^2$  and  $C_D$  is a constant (cp equation 2.2.4). Region Three must merge with Region Four and from equation 3.1.1 if  $C_D$  is constant,  $\theta_c$  is constant. The value  $Re_*^d = 1000$  as the beginning of the fourth region is probably only approximately correct but Shields' argument is consistent since the quadratic resistance law for spheres holds when  $Re_\infty^d > 10^3$  (Figure 1a).

We can deduce that for the fourth region the flow is fully turbulent near the bed as well as in the main body of the flow. That is, the 'gravel' is shedding strong eddies and the viscous sublayer is negligibly thin. Shields observed this behaviour as given in note 5 to the caption of Figure 1a.

Figure 2c shows that the value  $\theta_c = 0.06$ , suggested by Shields for the fourth region is near the upper limit of the threshold band whereas there are data points below the lower limit of the band. These are Neil's (1967) data for the movement of the occasional particle for which  $\theta_c$  maybe as low as 0.02. Neil's results are based on direct observation whereas Shields arrived at his threshold

band by extrapolating a measured sediment transport rate to a very small sediment transport rate. Shields, in fact, is not specific as to how small the transport rate should be for threshold. There is very little empirical evidence for the threshold criteria in the fourth region (Miller et al, 1977). The available evidence is also subject to criticism (Yalin, 1977) on the constraints to be used in determining the threshold (Section 3.3). The evidence from gravel transport measurements in upland streams (Carling, in press) must be treated with due caution since it is possible for  $h/d$  to tend to unity in these locations. Both Nikuradse and Shields warn that their results maybe invalid if  $h/d < 15$  or  $D/d < 15$ .

### 3.3 Specification of a threshold of sediment motion

Neil and Yalin (1969) were the first to publish an investigative study of the discrepancies found for the threshold criteria. Most experimenters adopt a visual criterion for threshold because a well-developed transport rate is not available for measure. This may be true for gravel transported by tides. A sediment load transport rate

$$q_s = 0 \text{ determined by extrapolating measured } q_s \text{ on a linear plot} \quad (3.3.1)$$

implies  $\theta = \theta_c$  whereas a visual criterion asserts

$$q_s = 0 \text{ and } \theta < \theta_c \text{ while } n = 0 \quad (3.3.2)$$

Where  $n$  is the number of grains displaced from a unit area of bed per unit time. The problem is what value should  $n$  take so that  $\theta = \theta_c$ . Neil and Yalin argue that if the investigator is not fully aware of the subjective nature of determining a visual threshold, condition (3.3.2) imposes a stricter threshold criteria for smaller grain sizes.

From considerations of kinematic similarity and dimensional analysis Neil and Yalin suggest that a number  $\epsilon$ , which allows for the effect of grain size, should be adopted conventionally to replace  $n$ ; that is,

$$\epsilon = nd^3/u_* = 1.0 \times 10^{-6} \quad (3.3.2)$$

Yalin (1977) has developed the discussion further by considering also the distribution of lift force fluctuations on the particle as measured by Einstein and El Sammi (1949). The detachment of a single particle from the bed is a stochastic process which also depends on particle shape, particle instability or degree of exposure. Yalin's discussion leads to a different interpretation for  $\epsilon$ ; that is,

$$\epsilon = \frac{q_s}{wl} \left( \frac{\rho d^5}{g(\rho_s - \rho)} \right)^{\frac{1}{2}} = \frac{n}{At} \left( \frac{\rho d^5}{g(\rho_s - \rho)} \right)^{\frac{1}{2}} \quad (3.3.3)$$

Thus, all investigators are urged to vary both the area  $A$  observed and the period of observation  $t$  so as to hold  $\epsilon$  constant. Miller et al (1977) have applied equation 3.3.3 to Paintal's (1971) data and determine  $\theta_c$  to equal 0.045 when  $Re_*^d$  is greater than 500. However, Miller et al had to adopt Einstein's (1950) saltation distance  $l$  equal to 100 grain units. We shall see that  $l$  is not a constant but increases generally as  $\theta$  increases (Section 5.0) and  $l = 100 d$  is too large for gravel if  $\theta < 1$ .

According to Miller et al (1977), values that have been proposed for  $\theta_c$  at large  $Re_*^d$  are 0.06, 0.047, 0.015, 0.009 and 0.007 (Shields, 1936; Zeller, 1963; Bogardi, 1965; Helland-Hansen, 1971 and Paintal, 1971). None of these proposed values have been determined within a standard constraint such as relations 3.3.3 and most values are probably individual observations of a random variable  $\theta_c$ .

#### 3.4 Alternatives to Shields' threshold band

In some circumstances it is disadvantageous to have  $u_*$  appearing in both abscissa and ordinate of Shields' graph. Shields himself provided additional graphs to circumvent this problem. To eliminate  $u_*$  from the abscissa, Yalin (1977) proposed

the combination  $(\sqrt{\Xi}, \theta)$  where  $\Xi = (Re_*^d)^2/\theta$ . Unfortunately, unlike  $Re_*^d$ , we cannot attribute any physical significance to  $\Xi$ .

Miller et al (1977), as with other marine scientists, offer an empirically determined threshold criterion of the form  $u_{100} = 160.0 d^{0.45}$  ( $d > 0.2$  cm) where the relative density is assumed to be 2.65. These forms should not be actively encouraged since their usefulness is specific and do not have the universality of Shields' band. Also, using a velocity scale different from  $u_*$ , such as  $\hat{u}$ , can sometimes lead to ambiguous, or even erroneous, conclusions. For example, see Yalin's (1977) discussion of Neil's (1967) depth-mean velocity sediment threshold criterion.

### 3.5 Calculated thresholds for different marine gravel sizes

It is instructive to determine that Shields' third and fourth regions are likely to be applicable to flat seabed gravel threshold conditions. Estimated values of  $\theta$  are given in Table 3 based on a typical maximum spring tide value of  $u_* = 5$  cm/s. The entrainment threshold number  $\theta_c$  has been estimated from Figure 2c using calculated values of  $Re_*^d$  for different gravel sizes. Only the  $\theta$  value for gravel (2-4 mm) appears to exceed the threshold value  $\theta_c$ . Moreover, the gravel fraction lies in Shields' third region ( $10 < Re_*^d < 1000$ ) where  $\theta_c \propto Re_*^d$  (Figure 2).

Because  $Re_*^d$  increases with  $d$  it is natural to anticipate that the marine gravel threshold lies predominantly in Shields' fourth region. Miller et al (1977), by collating existing data, have attempted to extend Shields' curve well into the fourth region but argue that measurements are too sparse to quote an unequivocal value  $\theta_c$  for this region. Indeed, Miller et al suggest that the fourth region begins at  $Re_*^d = 500$  whereas Shields, of course, says that begins at  $Re_*^d = 1000$  by analogy with  $Re_\infty^d = 1000$  (Figure 1a).

In the marine environment we are interested in any gravel movement whatever and Neil's results are pertinent to our investigation. For example, the critical friction velocity is 8.75 cm/s if  $d = 2$  cm and  $\theta_c = 0.02$ . This agrees well with the evidence of the occasional pebble being moved along the West Solent seabed at a value of  $u_* = 8.0$  cm/s based on velocity measurements in the upper flow.



#### 4.0 THE INFLUENCE OF NONUNIFORM GRAVELS ON THRESHOLD MOTION

According to Shields, if we plot the cumulative graph from a sieve analysis of mixed nonuniform sand sizes and find the modulus  $M$  of the curve is greater than  $1/3$  then the threshold condition  $\theta_c$ , on average, is the same as for uniform sand with a diameter  $d$  equal to the median diameter  $d_{50}$ . The modulus  $M$  is defined by

$$M = A_f/A_c \quad (4.0.1)$$

where  $A_c$ , associated with the coarse sediments, is the area bounded by  $d = 0$ ,  $\% = 50$ ,  $\% = 100$  and the cumulative curve.  $A_f$ , fine sediments, is the area similarly defined by the bounds  $d = 0$ ,  $\% = 0$ ,  $\% = 50$  and the cumulative curve. Shields says that most naturally occurring sand mixtures have moduli greater than  $1/3$ .

Shields proceeded on the assumption that the grain size distribution of all solid particles, such as the brown coal (0.35 mm-5.0 mm) used extensively in flume experiments, are such that  $M > 1/3$  and found that the threshold of nonuniform mixtures fell in close proximity with uniform mixtures.

Assuming that Shields is correct we can expect that his threshold band is invalid if  $M < 1/3$ . Without making any reference to Shields argument Einstein (1950) for example, says that  $d_{35}$  instead of  $d_{50}$  should be used in his (Einstein's) sediment transport formula. Swart (1976) suggests that a nonuniform sediment mixture should be split into several groups of fairly uniform grades and a formula, such as Ackers and White's formula, applied independently to each group.

#### 4.1 Bimodal sediment distribution

The discussion above generally applies to a unimodal sediment distribution only. This distribution, as a percentage of total weight, plotted against particle size has a single maximum. A bimodal distribution has two maxima with a minima between them, making three minima in all.

Certain sediment samples from the West Solent are bimodal (Dyer, 1972). The larger maximum is at the pebble or gravel size, and the smaller maximum is at the size of fine or medium sand. The centre minimum is at the size of coarse sand; that is about 1 mm. It is an interesting point that sedimentologically there appears to be a paucity of material at 2 mm (Russell, 1968). It is very probably that the bimodal distribution for the West Solent represents bedload and suspended load transport deposits. The current is periodic so that at slack water sand in suspension is deposited between the gravel fraction and not all of it is resuspended. Indeed, although pebbles are moved by these intense currents in sedimentological terms the pebbles must represent lag deposits. Alternatively, gravel can be moved as bedload near crests while sand is suspended near troughs. The resulting sediment is thus a mixture with the gravel particles not touching each other (Dyer, 1972). Although, in the West Solent case, the distinction between bed load and suspended sediment transport is marked by a bimodal distribution; for a unimodal distribution, this distinction inevitably becomes blurred. Nevertheless, several researchers attempt the distinction for unimodal distributions and some sediment transport formulae are designated as bed load only (Yalin, 1977).

## 5.0 INSTANTANEOUS HYDRODYNAMIC FORCES ON A SOLID PARTICLE

A knowledge of the second-by-second fluid forces that can act upon a fixed, non-rotating solid particle is useful background information to the problem of threshold solid particle motion. Many laboratory experiments have been carried out on gravel size particles in order to quantify the drag and lift forces present on a particle at the threshold, and during its initial movement.

The mean horizontal, or tangential, bed shear force, acting on a particle about to move is

$$\frac{\tau_0 d}{\eta} = \frac{\pi}{6} g(\rho_s - \rho)d^3 \tan \gamma \quad (5.0.1)$$

(White, 1940) where  $\gamma$  is the angle of repose. The 'horizontal' line of mean force ( $\tau_0$ ) intersects the gravitational force line (weight) at some point within the particle. The angle  $\gamma$  measures the angular displacement of a line through the

pivotal point on some neighbouring particle from the vertical line through the particle's centre-of-gravity.

According to White, when  $Re_*^d < 3.5$  particle tangential viscous forces are the dominant forces on a spherical particle. The interior intersection point lies above the CG because these forces act only on the upper exposed particle surface in a level bed. When  $Re_*^d \gg 3.5$ , the pressure forces are the dominant forces and these can be resolved at the CG as for normal pressure forces on a spherical body. It may be remembered from Section 2.7 that, according to Jackson, the bed shear stress appears to act at a height  $0.7k$  above the datum.

A vertical lift force acts upon the particle because of the acceleration of the flow over its upper surface. This is also likely to exist when the particle is a small distance from the boundary because of the difference in the velocities above and below the particle.

White (1940) attempted to demonstrate that a lift force was not operative by tying the particle to a thread in a horizontal plane. However, if the thread is taut and there is vertical motion then there must also be an upstream component of motion because the path of the particle would be circular.

Einstein (1950) and Yalin (1977) argue that the lift force is the most important force for initial particle displacement and their transport formulae are based upon this concept. Davies and Samad (1978) have measured the fluid dynamic lift on rigidly held non-rotating sphere. The sphere in this case, was 'lying' on a level bed of identical spheres and it was found that the lift is directed (negatively) towards the bed when the flow is hydraulically smooth ( $Re_*^d < 5$ ) and directed away from the bed when  $Re_*^d > 5$ .

Apperley (1968) has measured both the drag and lift forces in some of the most interesting detailed measurements available of fluctuating hydrodynamic forces on a pebble-sized particle (6.35 mm). The flow conditions were  $\hat{Re} = 186000$ ,  $Re_*^d = 417$  and  $u_* = 7.23$  cm/s. The flow was hydraulically rough by Nikuradse's criterion but by Shields' threshold criterion the third region is relevant where the viscous sublayer and hence viscous forces are still comparable with pressure forces. Figures 3 to 6 contain the main results of Apperley's work. In Figure 3 it is seen that the mean lift force is positive and  $1/2$  of the mean drag force when

the test sphere is a member of a level bed. Figure 4 shows that the rms value of the lift force is about 3/2 times the mean drag force when the sphere is raised 1/4 of its diameter from the bed. These measurements must then include the effect of the artificial gap below the sphere. Figures 3, 4 and 5 indicate that the peak fluctuating lift and drag forces are more than double the mean value when the relative degree of exposure is 1/4. An exposure of 1/4 means that the sphere is exposed a quarter diameter above the topmost points of the bed particles. Figure 6 is particularly interesting as it shows that the energy spectrum of the 3-component forces on a sphere with relative exposure  $z/d = 0.5$  is of the same general shape as a fluid turbulent energy spectrum for each component.

From Apperley's Figure 3 ( $Re_*^d = 417$ ), the lift force is just one-half the bed tangential drag force. Assuming a simple geometry where all forces intersect the CG of a spherical particle the immersed particle weight is effectively reduced such that

$$\text{Observed threshold } \tau_0 / \text{Calculated threshold } \tau_0 = 2/3 \quad (5.0.3)$$

White (1940) was unable to explain why the observed value of the threshold was systematically 1/2 of the value calculated from equation (5.0.1). His experimental range was  $33 < Re_*^d < 1280$  and included steel shot in water and sand in air.

White reported that instantaneous values of  $\tau_0$  varied by as much as 25%. Assuming the lift force is still 1/2 of the peak drag force: equation (5.0.2) becomes

$$\text{Observed threshold } \tau_0 / \text{Calculated threshold } \tau_0 = 10/11 \quad (5.0.3)$$

Thus, by reducing the effective immersed particle weight by a lift force, the observed and calculated threshold bed shear stress values are in good agreement.

Chepil (1959, 1961) results for instantaneous lift and drag forces on a sphere subjected to turbulent air currents are broadly in agreement with Apperley's

results. In particular, the lift force first increases and then decreases with height above the bed.

Bagnold (1974) was able to extend Apperley's results to a rotating cylinder moving relative to the bed by an ingenious experiment which allowed the observer and the 'saltating' particle to have the same fixed frame of reference. The bed was made to move as a conveyor-belt which sets-up a velocity profile in 'still' water by reason of the frictional contact between the bed and liquid.

Bagnold's results indicate that the lift force is less effective if the cylinder or sphere is allowed to rotate. The results are of interest generally for sediment transport problems but probably of limited value for marine gravel transport. The cylinder models a particle saltating fairly high in the flow, as observed by Francis (1973), and the ballistic nature of a single particle trajectory was confirmed. It is unlikely that tidally moved gravel would have anything but a very short, flat trajectory close to the bed. From flume measurements made by B Krishnappan (Yalin, 1977) the hop-length of gravel (2 to 4 mm) increases from about two gravel diameters at  $\theta = 0.45$  ( $Re_*^d = 400$ ) which is well above the threshold value (Figure 2) up to about seventy gravel diameters at  $\theta = 1$ .

## 6.0 SEDIMENT MOVEMENT THRESHOLD CRITERION FOR SURFACE WAVES ONLY

A review of the literature has been carried out by Davies and Wilkinson (1977) on the movement of non-cohesive sediment by surface water waves. Gravel transport by this agency, in deepwater, has seldom been observed in the sea. One reason for this is that surface wave induced bedforms at the scale of sand ripples (ie wavelength less than one metre) do not form if sediment is of gravel size. Yalin (1977) says that wedged-shaped sand ripples are one thousand times longer than grain size which means that gravel wavelengths cannot be shorter than two metres. According to Flemming and Stride (1967), however, if the sediment is a mixture of coarse sand (1 mm) and gravel (2-4 mm) long storm waves can induce large gravel-ripples about 1.25 m long in about 18 metres of water. The threshold of gravel movement in terms of the free stream orbital velocity and particle size is reproduced from Komar and Miller (1974) by Davies and Wilkinson.

The action of waves moving over a shingle bed has been simulated at full-scale in a Pulsating Water Tunnel (Hydraulics Research Station Note No 15, 1969). From this work, it is possible to predict the wave conditions necessary to move shingle or gravel of a particular size and known relative density, or conversely given the wave conditions, to determine the size of material of known relative density which will not be moved. A working diagram (Figure 7) illustrates the method for shingle of relative density 2.65. For limitations of pulsating water tunnels see Davies and Wilkinson (1977). Komar and Miller (1974) have converted the laboratory results for solid particle threshold movement in oscillatory flows so as to compare with the Shields-Rouse curve for threshold motion in steady unidirectional flow (Figure 2f). Because most of the measurements were made in a pulsating water tunnel or on an oscillating loose granular bed in still water, (evidently, these laboratory techniques cannot adequately model real waves) and since the conversion involves more than one stage, it is remarkable how close the data are to the Shields-Rouse curve in Shields' third and fourth regions. It has already been suggested in Section 2.2 that the relative velocity between bed particles and the fluid upstream may be more important than the presence of a wall boundary layer.

#### 6.1 Sediment movement threshold criterion for surface waves and tidal currents

According to Bijker (1967) the bed shear stress  $\tau_{\omega_0}$  due to a combination of waves and currents is given by

$$\tau_{\omega_0} = \tau_0 \left( 1 + \frac{1}{2} (0.45 \ln(h/z_0 - 1) u_{orb} / \hat{u})^2 \right) \quad (6.1.1)$$

Where  $u_{orb}$  is the orbital velocity amplitude near the bed and  $\tau_0$  is the bed shear stress on a level bed due to steady currents alone.

Price et al (1978) give the formula

$$\tau_{\omega 0} = \tau_0 + 2(\tau_0 \tau_{\omega})^{\frac{1}{2}} + \tau_{\omega} \quad (6.1.2)$$

Where  $\tau_{\omega}$  is the maximum bed shear stress due to waves only.

Equations 6.1.1 and 6.1.2 indicate, as expected, that the bed shear stress  $\tau_{\omega 0}$  is greater than either  $\tau_0$  or  $\tau_{\omega}$  taken separately.

The effectiveness of equation 6.1.1 for predicting sediment transport rates has been studied by Swart (1976). It must be emphasised, however, that this prediction can only be as good as the sediment transport formulae for steady unidirectional currents (Lees and Heathershaw, 1981). The predicted sediment transport rate given by the most popular formulae differ markedly; but surprisingly, using these formulae the computed resultant sediment directions over several tidal cycles are in close agreement (Heathershaw, 1981).

No evidence can be found that equation 6.1.2 has been tested in the marine environment but the effect of shoaling waves has received some attention. Novak (1972) has published tables to show that cobbles (14.3 cm) and boulders (27.1 cm) are displaced by waves generating a significant swash velocity. A significant swash velocity is the mean of the one-third highest velocities by analogy with the term-significant wave height. The distance displaced is not given and is assumed here to be some very small value, probably smaller than the particle radius. The observations were made during the summer when, presumably, the waves lacked the energy of winter storm waves. Novak concluded that the transport of coarse sediment in the swash zone agrees with the empirically derived Hjulstrom (1935) curves for shallow rivers.

Hjulstrom's curves are plots of threshold stream velocity such as  $\hat{u}$  or  $u_{100}$  against particle size. These curves are evidently different from Shields' curves. Shields' curves divide the graph into three regions: a region where particles are not displaced, a region where particles are displaced and a threshold band between them (Figure 2). Hjulstrom's graph consists of four regions: a region of scouring, a region of deposition, a threshold band similar to Shields'

threshold band and a transport region by suspensions where no scouring or deposition takes place. The transportation region lies below the velocity threshold band because the suspension has not yet settled out and the velocity is too low to cause erosion. Novak does not explain why his results agree with Hjulstrom's and it is difficult to see how suspended sediments might be related to the movement of cobbles and boulders. It is true, however, that bed-load transport can occur without serious scouring or accumulation taking place and in this sense Novak's results might be said to agree with Hjulstrom's graph since Novak's measurements fall mainly in the threshold and settlement regions.

It is obvious that there is a significant lack of understanding of the relationship of waves and currents acting together over a sediment bed particularly when bedforms are present.

#### 7.0 THE RELATION BETWEEN BED SHEAR STRESS AND ENGLISH CHANNEL SEDIMENTS

Preliminary results from a desk study (Price et al, 1978) indicate that 25 mm pebbles are likely to be mobilised by tidal currents off the Isle of Wight in 22 metres of water. A useful comparison (Figures 8 and 9) between sediment type and the mean bed shear stress, as derived from a numerical model, for the English Channel has been prepared by Pingree (1980). Excluding the Straits of Dover the largest bed shear stresses occur in the narrower section between the Cherbourg peninsula and the Isle of Wight. It is seen that the finer sediments have been swept away from the central narrowed part of the Channel in response to the tidal streams so that the lag deposits (gravel) and eroded rock are generally to be found North of the Cherbourg peninsula. In areas of decreasing bed shear stress sand, sandy mud, muddy sand and muds are successively encountered along a tidal transport path (Belderson et al, 1970). The English Channel mean bed shear stress distribution is sufficient to explain the sediment distribution although local sediment types differ in detail from the broad scheme.

#### 7.1 Biota growth on gravel as a measure of gravel stability

The presence of exofauna on gravel exposed to flowing sea-water is an indication of gravel stability. The growth and survival rate of exofauna might be used to



estimate how long the gravel has remained in a particular place. If biota is present uniformly over a large patch of gravel this would indicate that the bed shear stress is below threshold.

Underwater television observations are available which show that flora can be directly responsible for the transport of large rock fragments. Kelp acts as a drogue and drags large attached rock fragments very easily along a sandy seabed. It is likely that the rock was dislodged during a storm. Although gravel may be kelp-rafted (Emery et al, 1941) it is probable that this gravel represents a tiny fraction of gravel transported and deposited by more orthodox methods. However, near Selsey Bill, Sussex, UK the seasonal variation of weed-dragged stones, the predation of starfish on mussels, and other factors, appear to play a crucial role in the stability of pebble beaches and the pebble spit near the Bill (Wallace, 1971).

#### 8.0 SHORE PROTECTION, GRAVEL MOVEMENT AND EXTRACTION

Dredging criteria and the effects of gravel extraction on coastlines have recently been considered by Price et al (1978). However, brief details are given here for completeness.

If a section of coastline is destroyed suddenly after a long chain of events, both natural and by industrial exploitation, it is not uncommon for the dredging or gravel extraction industries to be blamed. The destruction of Hallsands fishing village is a well-documented example (Worth, 1904; 1909; 1923 and Hails et al, 1975). The dredging of Gt Yarmouth harbour is reputed to be responsible for the erosion of river banks some 10 miles inland. Numerous examples (eg Innes, 1977) can be cited but a long chain of cause and effect is extremely difficult to prove without an exhaustive scientifically based investigation. Indeed, since the natural mechanisms of change are, as yet, not fully understood few conclusions are arrived at without dissent.

Offshore gravel extraction may deprive a shingle beach of its source material. Whatever the size of the sediment for replenishable sediment transport to occur it must follow that either there is an inexhaustible sediment source or the transport paths are practically closed loops. Closed loops would be the case,

presumably, for a shingle beach embayed by rocky headlands. Changes must take place, of course, in geological time; aided in the short-term by catastrophic events such as storms.

After field trials to study the natural landward movement of pebbles Crickmore et al (1972) found that field tracer tests demonstrated both increase in bed mobility with decreasing depth and the existence of landward movement of gravel inshore of the 12 m depth. However, even at the two inshore sites the quantities of gravel transported towards the shore were found to be small, amounting to 1000 to 1500 cubic metres and less than 500 cubic metres per kilometre length of coast per annum from 9 to 12 m water depth, respectively. Dredging at these depths could interrupt the slow landward creep but the manifestation of this would be long-delayed. For instance, the tracer-centroid shift at the two sites indicate that the average pebble will take about 200 years to advance the 3 km from the 12 to 9 m contour. It is debatable whether changes on such a long time scale are significant when there is a strong probability that beach levels are controlled primarily by spatial and temporal variations in the littoral movement of shingle close inshore. However, at these depths beach changes arising from alteration of wave refraction might be the primary consideration. It was considered that gravel movements offshore of the 18 m contour along this piece of coastline (Worthing, Sussex) would be negligible at all times. Furthermore, at these depths the mass transport current (of surface waves) at the bed is too small to promote preferential landward drift.

Crickmore et al argue that shingle gained from the open sea is a small fraction of the supply eroded directly from cliffs and transported by longshore currents and waves. However, there will be an increasing tendency to protect cliffs from erosion as at Sheringham and Happisburgh on the Norfolk coast. This practice, together with offshore gravel extraction could starve some shingle beaches entirely

Kidson and Carr (1959) found that the maximum dispersal rate of pebbles parallel to the River Ore shingle spit near North Weis Point, Orford beach, Suffolk was 25.3 m/day although the maximum rate parallel to the spit 670 m offshore was 0.66 m/day with some tendency for pebbles to move landward. It has been extremely difficult to establish a casual link between shingle sorting and wave characteristics (Gleason and Hardcastle, 1971; Carr et al, 1970; Carr, 1974). We might suppose that this is because a curving beach is in quasi-equilibrium

with the dominant wave climate. The beach adopts a shape which is locally aligned with the dominant wave front. Once a shingle beach is in quasi-equilibrium there should not be a biased direction for shingle movement. Where there is a tendency for longshore sediment transport this is usually marked by some well-known geomorphological feature such as Gibraltar Point, Lincolnshire (King, 1972).

Locally increased water depths due to gravel extraction can alter the angle of incidence and increase the energy of waves onto a beach (Crickmore et al, 1972). The present state of knowledge indicates that the erosional effect of wave refraction onto English beaches is not negligible for holes dredged landward of the 18 m depth contour line (Motyka and Willis, 1974).

At the present time we can only infer the slow residual movement and direction of pebbles over the shelf sea floor from the asymmetry of gravel waves and by tracing the movement of radioactive pebbles at a few sites. It is necessary to corroborate these inferences by independent means such as the direct measure of flow rates and the application of gravel transport formulae.

## 9.0 SEDIMENT TRANSPORT FORMULAE

It is only within the past decade that sediment transport formulae have been used to predict the rates of marine sand transport and none have yet been verified for gravel in the sea. Assuming that the Swansea Bay tracer experiments (Heathershaw and Carr, 1977) were sufficiently accurate, the predictions fared badly compared with experimental results (Heathershaw and Hammond, 1979). Wave effects were not fully included in the predictions. Based on further experiments in the Sizewell-Dunwich sandbank area, Suffolk, UK (Lees and Heathershaw, 1981) all (five) predictions are consistently low at low tidal velocities and high at high tidal velocities. Consequently, Bagnold's formula, as reformulated by Gadd et al (1978), generally predicts the highest transported load and so appears to be satisfactory at low tidal velocities while Yalin's (1963) formula, which usually predicts the lowest transported sand load, is apparently satisfactory at high tidal velocities.

Yalin (1977) has argued that such discrepancies are sometimes the fault of the user because of failure to observe the limits of variables such as particle size, used to calibrate each formula. Except in the case of Yalin's own formula (see Appendix A.6) it is believed here that such limits have not been violated excessively in the above marine experiments and yet the agreement with experiment is very poor. Apart from wave action, there are several factors which may contribute to the discrepancies. For example, the value of  $u_*$  is required first and this is usually found by extrapolation of the velocity profile equation. As previously mentioned (Section 2.8) the prototype profile often deviates from such a profile due to unsteadiness in the flow, sediment suspensions or bedforms.

Fortunately, in compliance with Yalin's insistence, of the five formulae (Table 4) used previously by IOS (Taunton) only the Engelund-Hansen formulae has not been calibrated against the gravel (2-4 mm) fraction. Some of the formulae have been calibrated for pebble movement as well. Summaries of relevant formulae are given in Appendix A. The Swiss formula (A.5) is included because of its usefulness for quick calculations.

#### 9.1 Some considerations of sediment transport formulae

Bagnold's (1980) formula (Appendix A.2) is considered here for three reasons. Firstly, the formula is calibrated against the gravel fraction, secondly, Bagnold considers bimodal sediment distributions and thirdly, after many years of research into the subject Bagnold now says that sediment transport rates can only be determined by empiricism. Raudkivi (1976) also holds the view that a closed theoretical form for sediment transport rates is impossible at the present time. The author believes that a semi-empirical solution to the problem is possible and a thorough investigation of existing formulae should be carried out; retaining those parts which are sound theoretically and discarding the rest.

If the relative merits of the Ackers-White and Engelund-Hansen formulae (Appendices A.1 and A.4, respectively) are considered, it is found that the former has four empirical constants and the latter has only one. Thus, the former relies on empiricism more strongly and its success could well be due to sophisticated regression analysis. There are many curve-fitting exercises of this type, unlike the Ackers-White formula, some of these are constructed without any

theoretical considerations whatsoever (Raudkivi, 1976). In an appraisal of available methods, White et al (1978) say that the Engelund-Hansen formula is second only to the Ackers-White formula in predictive capability.

Raudkivi's (1976) account of the Engelund-Hansen formula would lead one to believe that it is only appropriate to dune-covered beds. This is not true, and it has been calibrated successfully against the sand fraction over a Froude number ( $\hat{u}/\sqrt{gh}$ ) range from 0.2 to about 1.5 (Yalin, 1977). This range is larger than for any other formula; for instance the Ackers-White formula is calibrated, like most formulae, over the Froude number range 0.2-0.8.

For comparisons of measured and predicted sediment transport rates in tidal currents which usually implies a Froude number range from zero to 0.2, Heathershaw (1981) finds that the Engelund-Hansen formula is not noticeably inferior to any other formula. Indeed, if the measurements of Lees and Heathershaw (1981) are also considered then, purely by ranking, the author finds that the Engelund-Hansen formula is the overall best predictor. Complications arise when the measurements of Lees and Heathershaw are included for consideration. The measurements are for a unimodal sand distribution and sediment is transported predominantly by suspensions. Now, with a unimodal distribution it inevitably becomes difficult to define the bed-load component of sediment transport. Yalin's formula is designated bed-load although its design is based upon the ballistic nature of sediment saltation. Lees and Heathershaw's results might be explained by a positively skewed sediment distribution as given by an excess of fines. Alternatively, the suspended sediments might contain wash-load which is material almost continually in suspension and not necessarily an in-situ sediment component. Lee and Heathershaw (1981) have considered only the bed-load transport component, and Engelund-Hansen's formula, as with the Ackers-White formula, predicts the total sediment mass transported.

Engelund-Hansen's formula is favoured by the author because it is based on energy principles (see Appendix A). Engelund-Hansen's (1967) similarity principle for dunes appears to have suffered a set-back from Yalin's (1977) critical assessment since Yalin's implies that Engelund-Hansen's skin friction and form drag proportions are not unique (see also Section 2.8). More importantly in the present context, Engelund-Hansen's formula has not been calibrated against the gravel fraction.

## 10.0 CONCLUSIONS

Despite some theoretical and experimental work on the problem of sediment transport by the combined action of waves and currents, many important questions remain unanswered. In this review the problem has been broken down into three parts - the movement of sediment by currents, shoaling waves and waves in deeper water. The movement of sediment by unidirectional currents has been studied extensively in the literature because of the importance of rivers for human settlement and agriculture. It has been indicated here that despite recent intensive investigation over some decades into the mechanisms for unidirectional sediment transport the agreement between prediction and observation is still poor. An accurate prediction of sediment movement by the combined action of waves and currents cannot be better than the best prediction for unidirectional currents alone. At the present time, (as a consensus) not one of the available sediment transport formulae has emerged as the best for predictive purposes.

The movement of gravel by waves and tides cannot be studied in isolation from the movement of, say, sand or mud. Indeed, gravel movement is, in some respects, an easier problem to solve. For typical river flows and shelf-sea tides, gravel invariably travels as bed-load only which is certainly not the case for sands. It has been suggested here that bimodal sediment distributions distinguish bed-load and suspended load (section 4.1). It seems that, in general, sediment grains (with relative density 2.65) greater than 1 mm in size are too heavy to travel far in suspension.

A great deal has been recorded in the literature about the movement of gravel in very shallow streams. Only one or two references (such as Carling, in press) were mentioned here because the author believes that Shields' threshold function is more appropriate to deep water marine conditions than it is very shallow streams (section 3.2). There may, however, be useful analogies to be drawn between the movement of gravel by shoaling waves and by shallow streams (section 6.1).

It has been mentioned in section 9.1 that Engelund and Hansen's (1967) formula should be singled out as a likely candidate for giving the best prediction for total sediment load transport. This semi-empirical formula appears to be the best overall predictor for sand transport. Unfortunately, this formula, it is

believed, has not yet been calibrated against the gravel fraction. This should not be a problem, since published data are available (eg Bagnold, 1980) against which Engelund and Hansen's formula can be tested. If this formula proves to be effective for gravel, as well as sand, this should set it apart from the other formulae for special study. Another aspect of this formula is that it attempts to exploit the distinction between bedform drag and bed 'skin' friction (section 2.8) and the 'skin' friction component is possibly a more important measurement for sediment transport.

Gravel-waves are of special interest in the general study of bedforms because certain kinds of bedforms, such as ripples, are formed by moving sands but not by moving gravels. It is, therefore, very useful to analyse gravel-waves and the flow characteristics appropriate to them with the anticipation that bedform types are accompanied by unique flow characteristics. In particular, it is an unanswered question why, within a width of about two miles of the West Solent, bands of gravel occur which are markedly different in wavelength and inter-banded with level gravels and sand-ribbons. To the north of these morphological provinces lie tidally exposed muds. Some answers are available, such as differential roughness inducing secondary circulations to explain sand ribbons (McLean, 1980) but a complete answer for all morphological provinces is still awaited.

Engelund and Hansen's sediment transport formula, like Einstein (1950) formula, does not have an explicit Shields' threshold criterion (Appendix A). A threshold criterion is, however, included implicitly. It may happen that, when the former formula is calibrated against gravel, a more explicit form of the threshold criterion (section 3.0) will be required. It may, therefore, be advantageous to recover Shields' original concept for a statistical interpretation for the threshold criteria and draw up probability curves of initial movement on Shields' graph. In which case, Yalin's work (section 3.3) and Einstein's statistical approach (Appendix A) should be a useful starting point for such a analysis.

Obviously, nothing can be proven about marine gravel transport without measuring gravel movement in real conditions together with the measurement of tide and wave flow characteristics. It is perfectly clear that, in the generally hostile marine environment, it is very difficult to make accurate measurements. It may be necessary, therefore, to continue to substantiate

hydraulically based predictions by geomorphological methods and other techniques (Heathershaw et al, 1981). Indeed, the study of biota growths (section 7.1) may prove that certain gravels have been immobile for a very long time.

Once the predictions of sediment movement under nearly steady unidirectional currents consistently acquire an acceptable degree of accuracy, it will be possible to return to the problem of sediment movement by waves and currents combined (section 6.1). Although the actual predicted quantities of sediment moved do not, in general, accord with measurement it is nevertheless true that the predicted directions of movement agree very closely with the geomorphological evidence. For instance, the general direction of sediment movement near sand banks conform with existing theories for sand bank stability in tidal flows. The existing evidence also suggests that although waves, in deeper water, may help to agitate sand into suspension it is predominantly tidal circulations that dictate sediment transport paths in UK waters (Heathershaw, 1981).

There is a pressing need for further research into the detailed process of gravel movement over the seabed and to improve the overall predictive capability for sediment transport in general. Such work, however, will necessarily need to incorporate the results of the detailed short-term small scale process studies (section 2.6 and section 2.8) into the framework of the larger scale and longer term processes.

#### ACKNOWLEDGEMENTS

I would like to thank A P Carr, K R Dyer, A D Heathershaw and D N Langhorne for their valuable contributions during the preparation of this report. I would like to acknowledge, also, the useful comments made by members of the Small-Scale Processes Team at IOS (Taunton) on a wide range of topics, such as waves and turbulence.



## REFERENCES

- ABRAMOWITZ, A and STEGUN, I A, 1965. Handbook of mathematical functions.  
New York: Dover, 1046 pp.
- ACKERS, P E and WHITE, W R, 1973. Sediment transport: new approach and analysis.  
Journal of the Hydraulics Division, American Society of Civil Engineers,  
99, (HY11), 2041-2060.
- APPERLEY, L W, 1968. The effect of turbulence on sediment entrainment.  
University of Auckland, New Zealand, PhD Thesis, 207 pp.
- BAGNOLD, R A, 1956. The flow of cohesionless grains in fluids. Philosophical  
Transactions of the Royal Society, B, 249, 235-297.
- BAGNOLD, R A, 1963. Mechanics of marine sedimentation. Pp 507-582 in The Sea,  
vol 3, edited by M N Hill. New York: Wiley-Interscience, 963 pp.
- BAGNOLD, R A, 1974. Fluid forces on a body in shear flow; experimental use of  
stationary flow. Proceedings of the Royal Society of London, A, 340,  
147-171.
- BAGNOLD, R A, 1980. An empirical correlation of bedload transport rates in  
flumes and natural rivers. Proceedings of the Royal Society of London,  
A, 372, 453-473.
- BELDERSON, R H, KENYAN, N H and STRIDE, A H, 1970. Holocene sediments on the  
continental shelf west of the British Isles. Institute of Geological  
Sciences Report No 70, 157-170.
- BIJKER, E W, 1967. Some considerations about scales for coastal models with  
moveable beds. Delft Hydraulics Laboratory Report No 50, 142 pp.
- BOGARDI, J L, 1965. European concepts of sediment transportation. Journal of  
the Hydraulics Division, American Society of Civil Engineers, 91, (HY1),  
29-52.
- CAILLEUX, A, 1965. Distinction des galets marins et fluviatiles. Bulletin de la  
Société géologique de France, 5, (15), 375-404.
- CALDWELL, D R and CHRISS, T M, 1979. The viscous sublayer at the sea floor.  
Science, 205, 1131-1132.
- CARLING, P A. In Press. The threshold of coarse sediment transport in broad  
and narrow natural streams: an extension to Shields 'diagram'.  
Earth Surface Processes.
- CARR, A P, 1974. Differential movement of coarse sediment particles. Pp 851-870  
in Proceedings of the 14th Coastal Engineering Conference, Copenhagen.  
June 24-28 1974, vol 2. New York: American Society of Civil Engineers.  
2647 pp in 4 vols.

- CARR, A P and BLACKLEY, M W L, 1969. Geological composition of the pebbles of Chesil Beach, England. Journal of Sedimentary Petrology, 41, 1084-1104.
- CARR, A P, GLEASON, R and KING, A, 1970. Significance of pebble size and shape in sorting by waves. Sedimentary Geology, 4, 89-101.
- CHARLTON, F G, 1977. An appraisal of available data on gravel rivers. Hydraulics Research Station Report No INT 151, 67 pp.
- CHANNON, R D and HAMILTON, D, 1971. Sea bottom velocity profiles on the continental shelf, south west England. Nature, 231, (5302), 383-385.
- CHEPIL, W S, 1959. Equilibrium of soil grains at the threshold of movement by wind. Proceedings. Soil Science Society of America, 422-428.
- CHEPIL, W S, 1961. The use of spheres to measure lift and drag on wind-eroded soil grains. Proceedings. Soil Science Society of America, 343-345.
- COLEBROOK, C F and WHITE, C M, 1937. Experiments with fluid friction in roughened pipes. Proceedings of the Royal Society of London, A, 161, 367-381.
- COLEMAN, N L, 1977. Extension of the drag coefficient function for a stationary sphere on a boundary of similar spheres. La Houille Blanche, No 4, 325-328.
- CRICKMORE, M J, WALKER, C B and PRICE, W A, 1972. The measurement of offshore shingle movement. Pp 1005-1025 in Proceedings of the 13th Coastal Engineering Conference, vol 2.
- DAVIES, A G, 1980. Field observations of the threshold of sand motion in a transitional wave boundary layer. Coastal Engineering, 4, 23-45.
- DAVIES, A G and WILKINSON, R, 1977. The movement of non-cohesive sediment by surface water waves: literature survey. Institute of Oceanographic Sciences Report No 45, 73 pp (unpublished manuscript).
- DAVIES, T R H and SAMAD, M F A, 1978. Fluid dynamic lift on a bed particle. Journal of the Hydraulics Division, American Society of Civil Engineers, 104, (HY8), 1171-1181.
- DYER, K R, 1969. Some aspects of coastal and estuarine sedimentation. Southampton University, Department of Oceanography, PhD Thesis. 102 pp.
- DYER, K R, 1971. The distribution and movement of sediment in the Solent. Southern England. Marine Geology, 11, 175-185.
- DYER, K R, 1980. Velocity profiles over a rippled bed and the threshold of movement of sand. Estuarine and Coastal Marine Science, 10, 181-199.
- EINSTEIN, H A, 1950. The bedload function for sediment transportation in open channel flows. United States Department of Agriculture, Soil Conservation Service, Technical Bulletin No 1026, 78 pp.

- EINSTEIN, H A and EL-SAMNI, 1949. Hydrodynamic forces on a rough wall. Review of Modern Physics, 21, (3), 520-524.
- EMERY, K O and TSCHUDY, R H, 1940. Transportation of rock by kelp. Bulletin of the Geological Society of America, 52, 855-862.
- ENGEL, P and LAU, Y L, 1980. Friction factor for two-dimensional dune roughness. Journal of Hydraulic Research, 18, 3, 213-228.
- ENGELUND, F and HANSEN, E, 1967. A monograph of sediment transport in alluvial streams. Technisk Vorlag, Copenhagen, 62 pp.
- FLEMMING, C A and HUNT, J N, 1976. A mathematical sediment transport model for unidirectional flow. Proceedings of the Institute of Civil Engineers, 61, (2), 297-310.
- FLEMMING, W C and STRIDE, A H, 1967. Basal sand and gravel patches with separate indicators of tidal current and storm wave paths, near Plymouth. Journal of the Marine Biological Association, 47, 433-444.
- FRANCIS, J R D, 1978. Experiments on the motion of solitary grains along the bed of a water stream. Proceedings of the Royal Society of London, A, 332, 443-471.
- GADD, P E, LAVELLE, J W and SWIFT, D J P, 1978. Estimates of sand transport on the New York shelf using near-bottom current meter observations. Journal of Sedimentary Petrology, 48, 239-252.
- GESSLER, J, 1971. Beginning and ceasing of sediment motion. Chapter 7, pp 7.1-7.22 in River Mechanics, edited by H W Shen. Fort Collins, Colorado: Colorado University Press.
- GLEASON, R and HARDCASTLE, P J, 1973. The significance of wave parameters in the sorting of beach pebbles. Estuarine and Coastal Marine Science, I, 11-18.
- HAILS, J R, 1975. Submarine geology, sediment distribution and quarternary history of Start Bay, Devon. Journal of the Geological Society, 131 (1), 1-5.
- HEATHERSHAW, A D and CARR, A P, 1977. Measurements of sediment transport rates using radioactive tracers. Pp 399-416 in Proceedings of Coastal Sediments '77 Conference, held Charleston, South Carolina. New York, American Society of Civil Engineers, 1133 pp.
- HEATHERSHAW, A D and SIMPSON, J H, 1978. The sampling variability of the Reynolds stress and its relation to boundary shear stress of drag coefficient measurements. Estuarine and Coastal Marine Science, 6, 263-274.

- HEATHERSHAW, A D and HAMMOND, F D C, 1979. Swansea Bay (Sker) project topic report: 6. Offshore sediment movement and its relation to observed tidal current and wave data. Institute of Oceanographic Sciences Report No 93, 119 pp (unpublished manuscript).
- HEATHERSHAW, A D, 1981. Comparison of measured and predicted sediment transport rates in tidal currents. Marine Geology, 42, 75-104.
- HEATHERSHAW, A D, CARR, A P and BLACKLEY, M W L, 1981. Swansea Bay (Sker) project topic report: 8. Final report: Coastal erosion and nearshore sedimentation processes. Institute of Oceanographic Sciences Report No 118, 67 pp. (unpublished manuscript).
- HELLAND-HANSEN, E, 1971. Time as a parameter in the study of incipient motion of gravel. Transactions of the American Geophysical Union. Northwest regional section, Corvallis, Oregon. Cited by Miller et al (1977) 507-527.
- HJULSTROM, F, 1935. Studies of the morphological activity of rivers such as illustrated by the River Fyris. Bulletin of the Geological Institution of the University of Upsala, 25, 221-527.
- HYDRAULICS RESEARCH STATION, 1969. Threshold movement of shingle in waves. HRS Notes, (15), 5-6.
- INNES, G, 1977. Solent bank, pot bank and Prince Consort dredging. Hydraulics Research Station Report No EX770, 28 pp.
- JACKSON, P S, 1981. On the displacement height in the logarithmic velocity profile. Journal of Fluid Mechanics, 111, 15-25.
- JEFFREYS, H, 1929. On the transport of sediment by streams. Proceedings of the Cambridge Philosophical Society. Mathematical and Physical Sciences, 25, 272-276.
- KELLING, G and WILLIAMS, P F, 1967. Flume studies of the reorientation of pebbles and shells. Journal of Geology, 75, 243-267.
- KIDSON, C and CARR, A P, 1959. The movement of shingle over the sea bed close inshore. Geographical Journal, CXXV, (3 and 4), 380-389.
- KING, C A M, 1972. Beaches and coasts. London: Edward Arnold, 570 pp.
- KINSMAN, B, SCHUBEL, J R, CARROLL, G E and GLACKIN-SUNDELL, M, 1979. A suggestion for anticipating alterations in wave action on shores consequent upon changes in water depths in harbours and coastal waters. State University of New York. Marine Science Research Centre, Special Report, No 27.

- KLINE, S J, REYNOLDS, W C, SCHRAUB, F A and RUNSTADLER, P W, 1967. The structure of the turbulent boundary layers. Journal of Fluid Mechanics, 30, 741-773.
- KNIGHT, D W and MacDONALD, D J, 1979. Hydraulic resistance of artificial strip roughness. Journal of the Hydraulics Division, American Society of Civil Engineers, 105, (HY6), 675-690.
- KOMAR, P O and MILLES, M C, 1974. Sediment threshold under oscillatory waves. Pp 756-765 in Proceedings of the 14th Coastal Engineering Conference, Copenhagen, vol 2.
- LANGHORNE, D N, 1981. An evaluation of Bagnold's dimensionless coefficient of proportionality using measurements of sandwave movement. Marine Geology, 43, 49-64.
- LEES, B J and HEATHERSHAW, A D, 1981. Sizewell-Dunwich banks field study topic report No 5. Institute of Oceanographic Sciences Report No 123, 113 pp (unpublished manuscript).
- MANTZ, P A, 1977. Incipient transport of fine grains and flakes by fluids extended Shields' diagram. Journal of the Hydraulics Division, American Society of Civil Engineers, 103, (HY6), 601-613.
- McLEAN, S R, 1981. The role of non-uniform roughness in the formation of sand ribbens. Pp 49-74 in Sedimentary Dynamics of Continental Shelves. Edited by C A Nittrouer. Amsterdam: Elsevier.
- MEYER-PETER, E and MULLER, R, 1948. Formulae for bed-load transport. Proceedings of the 2nd Congress of the International Association for Hydraulic Research, Stockholm. Cited by Yalin (1977), 113-117.
- MILLER, M C, McCAYE, I N and KOMAR, P D, 1977. Threshold of sediment motion under unidirectional currents. Sedimentology, 24, 507-527.
- MOTYKA, J M and WILLIS, D H, 1974. The effect of wave refraction over dredged holes. Pp 615-628 in Proceedings of the 14th Coastal Engineering Conference vol 1.
- NEILL, C R, 1967. Mean velocity criterion for scour of coarse uniform bed material. Proceedings of the 12th Congress of the International Association for Hydraulic Research, vol 3, Fort Collin, Colorado.
- NEILL, C R, 1968a. A re-examination of the beginning of movement for coarse granular bed materials. Hydraulic Research Station Report No INT 68, 37 pp.
- NEILL, C R, 1968b. Note on initial movement of coarse uniform bed material. Journal of Hydraulic Research, 6, (2), 173-176.

- NEILL, C R and YALIN, M S, 1969. Quantitative definition of beginning of bed movement. Journal of the Hydraulics Division, American Society of Civil Engineers, 95, (HY1), 585-587.
- NIKURADSE, J, 1933. Stromungsgesetz in rauher tohreu. VDI Forschungsarbeiten, No 361. Cited by Webber (1971), 84-86.
- NOVAK, I D, 1972. Swash-zone competency of gravel-size sediment. Marine Geology, 13, 335-345.
- PAINTAL, A S, 1971. A stocastic model for bedload transport. Journal of Hydraulics Research, 9, 527-553.
- PANG, Y H, 1939. Abhangigkeit der Geschiebebewegung von der Komifomn und der temperatur. Mitheilungen der Preussischen Versuchsanstalt fdr Wasserbau und Schiffbau, 37. Cited by Mantz (1977), 601-613.
- PETTIJOHN, F J, 1975. Sedimentary rocks. 3rd edition. New York. Harper and Row, 628pp.
- PINGREE, R D, 1980. p 424 in The north-west European shelf seas: the sea bed and the sea in motion, II, physical and chemical oceanography and physical resources. Edited by F T Banner, M B Collins and K E Massie. Amsterdam: Elsevier, 638 pp.
- PRICE, W A, MOTYKA, J M and JAFFREY, L J, 1978. The effect of offshore dredging on coastlines. Pp 1347-1358 in Proceedings of the 16th Coastal Engineering Conference, vol 2.
- RAUDKIVI, A J, 1976. Loose boundary hydraulics. 2nd edition. Oxford: Pergamon, 397 pp.
- SARKISIAN, S G and KUMOVA, L T, 1955. Orientation of pebbles and methods of studying them for paleogeographic construction. Izvestia Academy of Sciences USSR. Cited by Pettijohn (1975), pp 68-69.
- SCHOKLITSCH, A, 1914. Uber schleppkraft und Geschiebebewegung. Engelman, Leipzig. Cited by Mantz (1977), 601-613.
- SHIELDS, A, 1936. Application of similarity principles and turbulence research to bed-load movement. Translated from Anwendung der Aehnlichkeits Geschiebebewegung, in: Mitteilungen der Preussischen Versulliodunstalt fur Wasserbau und Schiftbau. Berlin, by W D Ott and J C von Vcheten. Pasadena: California Institute of Technology Hydrodynamics Laboratory Publication No 167, 36 pp.
- SMITH, J D, 1977. Modelling of sediment transport on continental shelves. Pp 539-577 in The Sea, vol 6, edited by E D Goldberg, A E Maxwell and M N Hill. New York: Wiley, 1084 pp.
- SMITH, J D and McLEAN, S R, 1977. Spatially averaged flow over a wavy surface. Journal of Geophysical Research, 82, (12), 1735-1746.

- SOULSBY, R L, 1980. Selecting record length and digitization rate for near-bed turbulence measurements. Journal of Physical Oceanography, 10, (2), 208-219.
- SOULSBY, R L and DYER, K R, 1981. The form of the near-bed velocity profile in a tidally accelerating flow. Journal of Geophysical Research, 86, (C9), 8067-8074.
- STANLEY, D J and SWIFT, D J P, editors, 1976. Marine Sediment Transport and Environmental Management. New York; Wiley, 602 pp.
- STERNBERG, R W, 1968. Friction factors in tidal channels with differing bed roughness. Marine Geology, 6, 243-260.
- SUNDERMANN, J, HOLLMERS, H and PULS, W, 1978. The influence of dune and flow parameters on the friction factor. Pp 1787-1800 in Proceedings of the 16th Coastal Engineering Conference, vol 2, Hamburg.
- SWART, D H, 1976. Coastal sediment transport. Delft Hydraulics Laboratory Report No R968, 61 pp.
- TAYLOR, B D and VANONI, V A, 1972. Temperature effects in low-transport, flat bed flows. Journal of the Hydraulics Division, American Society of Civil Engineers, 98, (HY8), 1427-1445.
- TRITTON, D J, 1977. Physical fluid dynamics. New York: Van Nostrand Reinhold Company Limited. 352 pp.
- WALLACE, H, 1971. A preliminary investigation into the part played by marine plants and animals in the movement of shingle over the seabed and on and off beaches with particular reference to the Selsby Bill area. Report to the British Sub Aqua Club, Kingston upon Thames Branch, 51 pp (unpublished manuscript).
- WANG, K C and WILSON, R E, 1979. An assessment of the effects of bathymetric changes associated with sand and gravel mining on tidal circulation in the lower bay of New York harbour. State University of New York, Marine Science Research Centre, Special Report No 18.
- WEBBER, N B, editor, 1971. Fluid mechanics for civil engineers. London: Chapman and Hall, 340 pp.
- WORTH, R H, 1904. Hallsands and Start Bay. Report and Transactions of the Devonshire Association for the Advancement of Science, 36, 302-346.
- WORTH, R H, 1909. Hallsands and Start Bay: Part II Report and Transactions of the Devonshire Association for the Advancement of Science, 41, 301-308.
- WORTH, R H, 1923. Hallsands and Start Bay: Part III. Report and Transactions of the Devonshire Association for the Advancement of Science, 55, 131-147.
- WHITE, C M, 1940. The equilibrium of grains on the bed of a stream. Proceedings of the Royal Society of London, A, 174, 323-338.

- WHITE, W R, 1972. Sediment transport in channels: a general function. Hydraulics Research Station Report No INT 104, 25 pp.
- WHITE, W R, MILLI, H and CRABBE, A O, 1978. Sediment transport theories: an appraisal of available methods (2 volumes). Hydraulics Research Station Report No IT 119, 101 pp.
- WILKINSON, R H, 1980. Swansea Bay (Sker) project topic report: 7. Foreshore sediment movement and its relation to observed tidal currents and wave climate. Institute of Oceanographic Sciences Report No 98, 38 pp.
- YALIN, M S, 1963. An expression for bed-load transportation. Journal of the Hydraulics Division, American Society of Civil Engineers, 89, (HY3), 221-250.
- YALIN, M S, 1964. On the average velocity of flow over a moveable bed. La Houille Blanche, 1964 No 1. Cited by Yalin (1977) p 276.
- YALIN, M S, 1977. Mechanics of sediment transport (2nd edition). Oxford, Pergamon, 298 pp.
- ZELLER, J, 1963. Einführung in den Sedimenttransport an fließenden Gerinnen. Schweiz, Bauzeitung, Jg 81, 597-602. Cited by Miller et al (1977), 507-727.



TABLE 1

The Wentworth-Udden size classification.

Particle	Size Range
Boulder	Greater than 256 mm
Cobble	64 mm - 256 mm
Pebble	4 mm - 64 mm
Gravel	2 mm - 4 mm
Sand	1/16 - 2 mm
Silt	1/256 - 1/16 mm
Clay	Less than 1/256 mm

Table 2: A comparison of physical roughness height  $k$  and the zero-velocity surface height  $Z_0$  above datum for a range of surface textures:

- (a)  $Z_0$  determined by extrapolating the velocity profiles;
- (b) the order of magnitude discrepancy in the stated and extrapolated values of Einstein and El Sammi's  $Z_0$  may be due to incorrect labelling of their velocity diagram.

	Nikuradse (1933)	Schlichting (after White 1940)	Einstein and El Sammi (1949)	Chepil (1961)	Grass (1977)	
Surface texture	Uniform 'rounded' sands of diameter $d$ packed tightly together in a single layer.	Spheres of diameter $d$ fixed to flat plate in grid pattern with $1.5 d$ spacing.	6.9 cm diameter plastic hemispheres fixed hexagonally to bottom of flume.	Levelled 0.3 cm pebbles or pebble mounds 0.8 cm or 5.0 cm high.	Levelled coarse sand of diameter 0.2 cm or levelled 0.9 cm pebbles on flume bottom.	
Adopted datum	Inside surface of 'smooth' pipe.	Surface of flat plate in contact with spheres.	Flat surface of hemispheres fixed to flume.	Mean level of pebble/air interface.	Bottom of flume.	
Fluid characteristics	Hydraulically rough.	Hydraulically rough.	Hydraulically rough.	Air	$Re_*^k = 20.7$ $\hat{Re} = 6700$ (transitional)	$Re_*^k = 84.2$ $\hat{Re} = 6620$ (rough)
Physical roughness height $k$ above datum	$k = d$	$k = d$	Height of hemisphere $k = d/2$ $= 3.45 \text{ cm.}$	The radius of test sphere laid in pebbles $k = d/2$ $d = 0.3 \text{ cm}$ $d = 0.8 \text{ cm}$ $d = 5.1 \text{ cm}$	$k = 0.213 \text{ cm}$ $k = 1.07d$	$k = 0.762 \text{ cm}$ $k = 0.85d$
Effective zero-velocity surface height $Z_o$ above datum.	Determined semi-empirically $Z_o = k/33$ (Webber, 1971)	Determination unknown $Z_o = k/9$	As stated (b) $Z_o = 2.2 \text{ cm}$ $Z_o = 0.64 k$ (a) $Z_o = 0.24 \text{ cm}$ $Z_o = 0.07k$	(a) $Z_o = 0.2 k$	(a) $Z_o = 0.127 \text{ cm}$ $Z_o = 0.6 k$	(a) $Z_o = 0.62 \text{ cm}$ $Z_o = 0.8 k$

TABLE 2

	GRAVEL	SMALL PEBBLES	LARGE PEBBLES
d (mm)	3	10	50
$Re_*^d$	150	500	2500
$\theta$	0.051	0.015	0.003
$\theta_c$	0.02-0.06	0.02-0.07	0.02-0.07

Table 3: A comparison of Shields' entrainment number and Shields' threshold band (Fig 2c) for  $u_* = 5$  cm/s and the particle sizes given.

TABLE 4

Originators		Date	Transport Mode
Ackers and White	abd	1973	total load
Bagnold		1980	bedload
Einstein	cd	1950	bedload
Engelund-Hansen	abd	1967	total load
Meyer-Peter and Müller		1948	bedload
Yalin	cd	1963	bedload

Used recently by a: Swart (1976);

b: Flemming and Hunt (1976);

c: Gadd et al (1978)

d: Heathershaw and Hammond (1979) and  
Lees and Heathershaw (1981).

Note: In the case of gravel transport is to be expected that the total load is the same as bedload unless the sediment distribution is bimodal.

## APPENDIX

### A.0 A COMPARISON OF FORMULAE USED IN SHELF-SEA STUDIES

Regional marine sediment transport budgets (Table 4) have been analysed for the New York Shelf (Gadd et al, 1978); Swansea Bay, South Wales (Heathershaw and Hammond, 1979) and the Sizewell-Dunwich area off the Suffolk coast, England (Lees and Heathershaw, 1981). Compared with the other formulae, Yalin's bedload formula under predicted sand transport rates at higher tidal velocities. The sediment type at each site was generally near the fine sand fraction. Although Gadd et al found it necessary to reformulate Bagnold's (1956, 1963) formulae and recalibrate Einstein's (1950) formula they did not do either for Yalin's version for calculating the sediment transport rate (Heathershaw, 1981). During the preparation of this report, the author discovered that all three formulae used by Gadd et al were originally calibrated against the gravel fraction (Yalin, 1977). Consequently, Yalin's empirical constant 0.635 could easily be inappropriate for fine sand and this may explain its general tendency to underpredict sand transport rates at higher flow velocities.

Because of coastal configuration and shelf conditions maximum tidal stream velocities at the three sites increase in the order - New York Shelf, Swansea Bay and Sizewell-Dunwich respectively. The reason why Bagnold's formula as reformulated by Gadd et al (1978) tends to overpredict sand transport rates, compared with other formulae, needs further consideration.

Because the best sediment transport measurements are those available from controlled flume experiments it follows also that most calibrations are made over the Froude number range 0.2-0.8. The Froude number range for shelf-seas and deep rivers is from zero to about 0.2. Consequently, although a zero Froude number ( $\hat{u}/\sqrt{gh}$ ) is, evidently, possible in a flume - for strict parity, calibrations ought to be done in deep water within this lower range. The conditions and instruments are such, however, that only very approximate measurements can be made. A provisional list (Table 4) of extant formulae are reviewed briefly as follows.

## A.1 ACKERS AND WHITE'S (1973) TOTAL LOAD FORMULA

It is beyond the scope of this report to review in full the derivation of Ackers and White's formula. Full details of the theory and calibration techniques can be found elsewhere, eg White (1972), Ackers and White (1973), White et al (1975,1978). The general function of Ackers and White is based on the physics of the stream power concept (see A.2 and A.4) and dimensional considerations, and is expressed in terms of three dimensionless groups as follows:

$$G_{gr} = C \left\{ \frac{F_{gr}}{A} - 1 \right\}^m \quad \text{A.1.1}$$

Where  $G_{gr}$  is the dimensionless sediment transport given by:

$$G_{gr} = \frac{c \rho h}{\rho_s d_{35}} \left( \frac{u_*}{\hat{u}} \right)^n \quad \text{A.1.2}$$

Here  $c$  is the concentration by weight of sediment which is related to the total load transport rate  $q_{st}$  by  $q_{st} = c u/g$ .  $F_{gr}$  is a dimensionless mobility number given by:

$$F_{gr} = \frac{u_*^n}{(g d_{35} (\frac{\rho_s}{\rho} - 1))^{\frac{1}{2}}} \left( \frac{\hat{u}}{2.46 \ln(10h/d_{35})} \right)^{1-n}$$

For coarse sediments the coefficients take values  $A = 0.17$ ,  $C = 0.025$ ,  $m = 1.50$  and  $n = 0.0$ .

Important points to note about Ackers and White's formula are:

- a) although it was calibrated against 1000 data sets these were mostly for flow depths less than 0.4 m;
- b) the formula may be applied to particle sizes in the range 0.04-4.0 mm;
- c) the equation is based upon experiments in which there was established sediment motion and the equations forecast initial movement conditions which give reasonable agreement with previous threshold studies;
- d) the equation is not sensitive to bedform and may be applied to plane, rippled and duned configuration for Froude numbers  $0.2 < F < 0.8$ ;
- e) the equation incorporates a transition exponent  $n$  which affects the change from friction velocity ( $u_*$ ) to depth mean flow ( $\hat{u}$ ) through intermediate particle sizes.

## A.2 BAGNOLD'S (1980) BEDLOAD FORMULA

Bagnold's formula is a purely empirical expression of the form

$$q_{sb} \propto (\tau_0 \hat{u} - \tau_c \hat{u}_c)^{\frac{3}{2}} h^{-\frac{2}{3}} d^{-\frac{1}{2}} \quad \text{A.2.1}$$

where  $\tau_0 \hat{u}$  has the dimensions of power per unit plan area. The threshold stream power  $\tau_c \hat{u}_c$  is the value of  $\tau_0 \hat{u}$  at which sediment begins to move. Stream power is a useful concept since the sediment can be considered as a load and the stream as a machine for transporting this load. Because Bagnold has introduced the relation A.2.1, which is significantly different from his well-known (1956) bedload formula (Yalin, 1977; Heathershaw, 1981), one can only assume that earlier formulae are superseded. The stream power concept of earlier formulae was expressed as  $\tau_0 u_*$  (see A.4)

Expression A.2.1 is dimensionally incomplete but it can be made dimensionless by dividing each parameter by any standard set of values chosen from reliable experimental data as depicted by the hashed values in the following expression

$$\frac{q_{sb}}{q_{\#}} \propto \left\{ \frac{\tau_0 \hat{u} - \tau_c \hat{u}_c}{(\tau_0 \hat{u})_{\#} - (\tau_c \hat{u}_c)_{\#}} \right\} \left\{ \frac{h}{h_{\#}} \right\}^{-\frac{2}{3}} \left\{ \frac{d}{d_{\#}} \right\}^{-\frac{1}{2}} \quad \text{A.2.2}$$

For reasons given in section 9.1 the author is of the opinion that this purely empirical approach is retrogressive. Bagnold's important stream power concept, however, is retained and the other two parameters raised to negative powers are challenging and fruitful concepts for debate. Bagnold also consider bimodal sediment distributions. The author is of the opinion that sediment transport problems concerning these sediment types should be treated as bedload and suspended load. It may be sufficient to apply two characteristic particle sizes to distinguish bedload from suspended load and apply a formula, such as Engelund and Hansen's formula, to each characteristic size.



### A.3 EINSTEIN'S (1950) BEDLOAD FORMULA

Because a detailed critical analysis is given in Yalin (1977) only a brief outline of this formula is given here. Einstein's equation differs from others in a number of ways. These are:

- (a) the equation is stochastic and relates sediment transport to random velocity fluctuations rather than mean flow parameters;
- (b) the equation contains an implicit threshold criterion for sediment movement.

According to Einstein's equation the initiation of particle motion occurs when the instantaneous lift forces are greater than the immersed weight of sediment. The probability (P) of this occurring is given by the normal error law:

$$P = 1 - \frac{1}{\pi^{1/2}} \int_{-B_* \psi_*^{-1} / \eta_0}^{B_* \psi_*^{-1} / \eta_0} e^{-t^2} dt \quad \text{A.3.1}$$

where  $\eta_0 = 0.5$  and  $B_*$  is a constant  $\psi_*$  is the flow intensity which is simply the inverse of Shields' entrainment number and given by:

$$\psi_* = g \left( \frac{\rho_s - \rho}{\rho} \right) \frac{d_{s0}}{u_*^2} \quad \text{A.3.2}$$

Bedload transport  $q_{sb}$  is thus expressed in terms of a dimensionless sediment transport  $\phi$  given by:

$$\phi = \frac{q_{sb}}{\rho_s} \left( \frac{\rho}{\rho_s - \rho} \cdot \frac{1}{gd_{s0}^3} \right)^{1/2} \quad \text{A.3.2}$$

which is related to the probability of particle motion P by:

$$\frac{P}{1-P} = A_* \theta \quad \text{A.3.4}$$

where  $A_*$  is a constant. Thus, the bedload transport may be expressed in terms of  $P$  and  $A_*$  as:

$$q_{sb} = \frac{P}{1-P} \cdot \frac{\rho_s}{A_*} \left( \frac{\rho_s - \rho}{\rho} \cdot g d_{50}^3 \right)^{\frac{1}{2}} \quad \text{A.3.5}$$

Einstein obtained the constants  $A_* = 43.5$  and  $B_* = 0.143$  from flume data for coarse particle sizes  $d_{50}$  of 0.7 mm and 28.6 mm.

To calculate  $q_{sb}$  from (A.3.5) it is necessary to evaluate the integral (A.3.1). This can be done using a rational approximation (see Abramowitz and Stegun, 1965).

#### A.4 ENGELUND AND HANSEN'S (1967) TOTAL LOAD FORMULA

It is commonly supposed that the effects of skin friction and form drag can be represented by single parameters  $\tau_0'$  or  $\theta'$  and  $\tau_0''$  or  $\theta''$  respectively so that total mean bed shear stress  $\tau_0$  is given by

$$\tau_0 = \tau_0' + \tau_0'' \text{ or } \theta = \theta' + \theta'' \quad \text{A.4.1}$$

The effects of suspended sediments will be ignored here but see Yalin (1977) for further details of equations A.4.1. The available stream power per unit plan area for sediment transport is  $(\tau_0' - \tau_c') u_*$  where  $\tau_c'$  is the value of  $\tau_0'$  in  $\theta_c'$ . For wedge-shaped dunes, say, of length  $L$ , the work done by stream power through the distance  $L$ , lifts a sediment volume  $V$  per unit width per unit time through the dune height which is twice the amplitude  $a$ . The authors of the formula assume that

$$2ag(\rho_s - \rho)V \propto L(\tau' - \tau'_c)u_* \quad \text{A.4.1}$$

or

$$\lambda V \left( \frac{2a}{\lambda L} \right) \propto \frac{\tau' - \tau'_c}{g(\rho_s - \rho)d} \cdot u_* d \quad \text{A.4.2}$$

Where  $\lambda = 2u_*^2/\hat{u}^2$  is the value of the friction factor assumed by Engelund and Hansen (Yalin, 1977). The relation A.4.2 can be written as

$$\lambda V \left( \frac{2a}{\lambda L} \right) \propto (\theta' - 0.06)\theta^{\frac{1}{2}} \left( \frac{\rho_s}{\rho} - 1 \right) g d^3)^{\frac{1}{2}} \quad \text{A.4.3}$$

Where Engelund and Hansen, evidently, used Shields' threshold value on a plane bed for the fourth region; that is,  $\theta'_c = \theta_c = 0.06$ . The dimensionless sediment discharge  $\emptyset$  is defined by

$$\emptyset = V / (g(\frac{\rho_s}{\rho} - 1)d^3)^{\frac{1}{2}} \quad \text{A.4.4}$$

From the rules of similarity for models with distorted vertical scales, Engelund and Hansen deduce that  $2a/\lambda L$  is a constant although Yalin (1977) argues that similarity principles do not lead to a unique solution. Assuming however,  $2a/\lambda L \approx \text{constant}$ , relation A.4.3 becomes

$$\lambda \emptyset \propto (\theta' - 0.06)\theta^{\frac{1}{2}} \quad \text{A.4.5}$$

From data analysis, Engelund and Hansen find that  $\theta' - 0.06 = 0.4\theta^2$  so that

$$\lambda \emptyset \propto \theta^{\frac{5}{2}} \quad \text{A.4.6}$$

The coefficient of proportionality is 0.1 when fitted to flume total load transport rates with grain size range  $0.19 \text{ mm} < d < 0.93 \text{ mm}$  and Froude number range  $0.2 < F < 1.5$ .

Thus, the experimental range of bedforms included ripples, dunes, stationary antidunes, antidunes and chute-and-pool. This is an exceptionally good result for a semi-theoretical approach which involved the friction factor. The authors of the formula find that good predictions are obtained providing nonuniform sediments do not include a large proportion of fines; that is,  $d$  is not less than 0.15 mm.

#### A.5 MEYER-PETER and MULLER (1948) BEDLOAD FORMULA

The "Swiss formula" is included here because it is simple, and therefore useful for quick calculations, and it has an explicit threshold criterion. The formula has been calibrated within the following parameter limits.

- a)  $1 \text{ cm} < h < 120 \text{ cm}$ ;
- b)  $0.0004 < i < 0.02$ ;
- c)  $0.4 \text{ mm} < d_{50} < 30 \text{ mm}$ ; and
- d)  $0.25 < \rho_s < 3.2$

After Yalin (1977) the formula is given by

$$\phi = \frac{q_{sb} \rho}{(g \rho_s d)^{\frac{3}{2}}} = 8(\theta - 0.047)^{\frac{3}{2}} \quad \text{A.5.1}$$

which implies yet another constant threshold value  $\theta_c = 0.047$ .

#### A.6 YALIN'S (1963) BEDLOAD FORMULA

In Yalin's theory particles are assumed to move over a flat bed in a ballistic manner. The formula is calibrated against the 'gravel' fraction (0.8 mm to 28.6 mm) and so it is supposed that particle trajectories are small and close to the bed. Therefore, the formula is designated as bedload. The bedload transport rate is given by:

$$q_{sb} = 0.635 \rho_s d_{50} u_*^3 \left(1 - \frac{1}{as} \ln(1 + as)\right) \quad \text{A.6.1}$$

where

$$a = 2.45 \left(\frac{\rho}{\rho_s}\right)^{0.4} \theta_c^{\frac{1}{2}}$$

and

$$s = \frac{\theta}{\theta_c} - 1 = \frac{\tau_0}{\tau_c} - 1$$

Yalin (1977) finds, using his formula, that the threshold for 28.6 mm pebbles, 5.2 pebbles and 0.7 mm sand is 0.046 and 0.033 respectively. Gadd et al (1978) found that equation A.6.1 gave good results for sand diameter  $d_{50} = 0.19$  mm near threshold but underestimated sand transport rates at higher velocities.

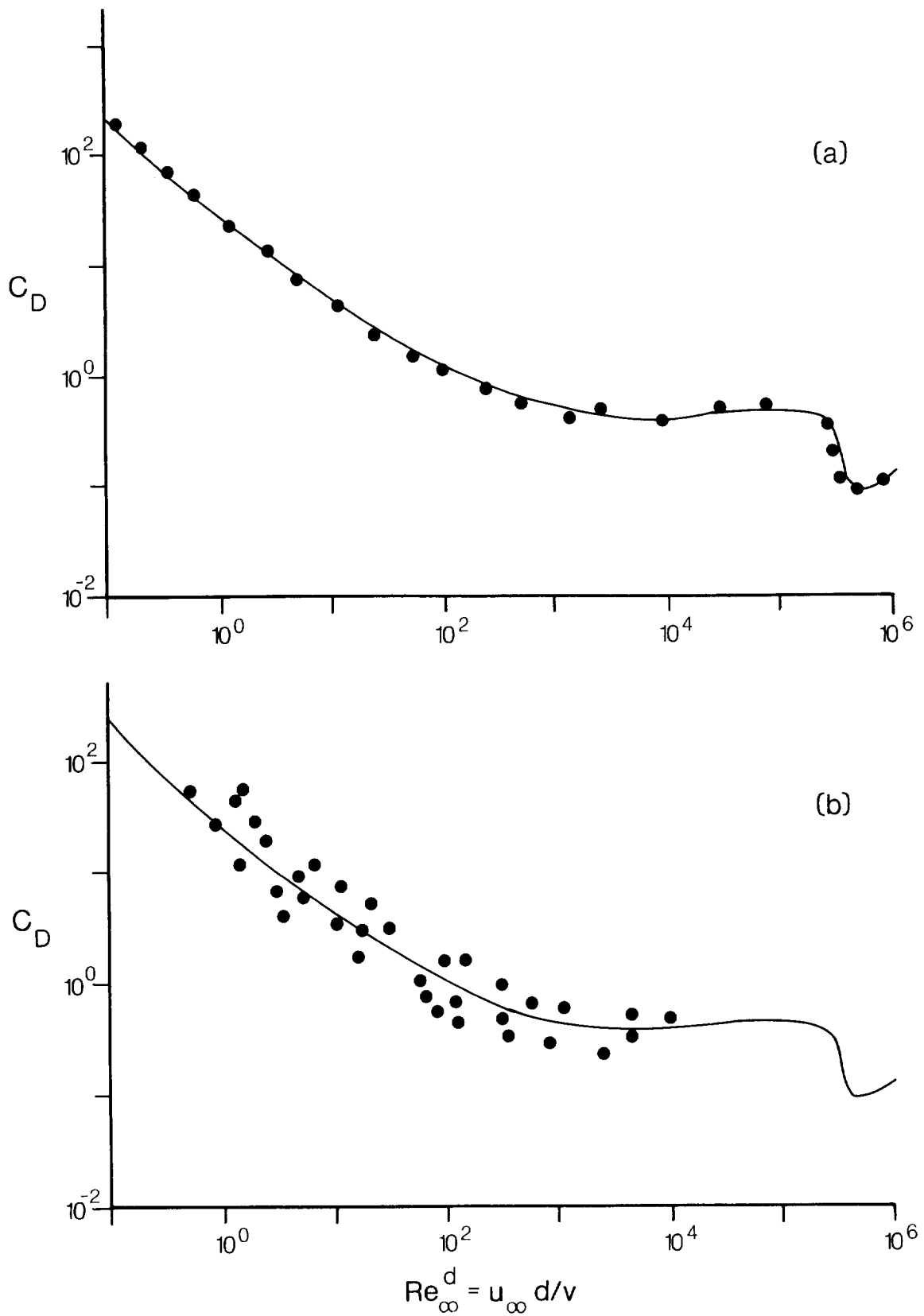


Fig 1: (a) Variation of drag coefficient with Reynold's number for a sphere in boundless fluid flow; (b) variation of drag coefficient with Reynold's number near a rough wall as compared with the curve in (a) (after Coleman, 1977).

Fig 2: According to their authors the stippled bands in (c) and (d) are up-to-date versions of Shields' threshold band in (a). The curve in (f) is the mean position, or Shields-Rouse threshold function, of Shields' threshold band. The curves in (b) and (e) are the best single line fit to the authors' measurements and no attempt is made here to distinguish the earlier measurements used as corroborative evidence by these authors. For clarity, not all the available data points are plotted. Measurements which are of particular relevance here are shown as open circles or asterisks.

(a) The stippled region shows the threshold of solid particle motion as determined, presumably, by extrapolating the sediment transport rate curve plotted on log-log paper. Different bedform morphology was observed at values of  $Re_d^*$  and  $\theta$  as numbered:

1. Ripples
2. Scales (short bars)
3. Oblique bars (long bars)
4. Flat bed elevations
5. Developed roughness flow about the grain
6. Gradual shortening and deepening of bed formation
7. Saltation over crests and
8. Abrasion.

(after Shields, 1936)

A modern classification of morphological types and hydrodynamic conditions might be:

1. Ripples
2. Three dimensional short dunes
3. Three dimensional long dunes
4. Lower stage flat bed
5. Bed grains shedding eddies
6. Dunes developing stronger lee eddies
7. Suspended sediment transport developing at dunes crests and
8. Upper stage flat bed.

(b) The best fitting threshold function for sediment motion as determined by varying fluid temperature and other parameters.

(after Taylor and Vanoni, 1972)

(c) The best fitting threshold band for sediment motion as determined by carefully vetting and collating available measurements. The open circles are based on Neil's (1967) measurements.

(after Miller et al, 1977)

(d) The stippled region is the threshold band for rounded solid grain motion. The open circles are based on measurements using natural slates with interstitial fill (after Pang, 1939). The asterisks are for natural slates without interstitial fill (after Schoklitsch, 1914).

(after Mantz, 1977)

Fig 2: (e) The best fitting solid particle threshold curve as determined by (Contd) the authors' own measurements and earlier published measurements. The open positions are based on Neil's (1967) measurements.

(after Yalin and Karahan, 1979)

(f) The threshold values of solids in oscillatory stream flows simulating the behaviour of wind-wave induced orbital motion as compared with the Shields-Rouse threshold curve for unidirectional flows.

(after Komar and Miller, 1974)



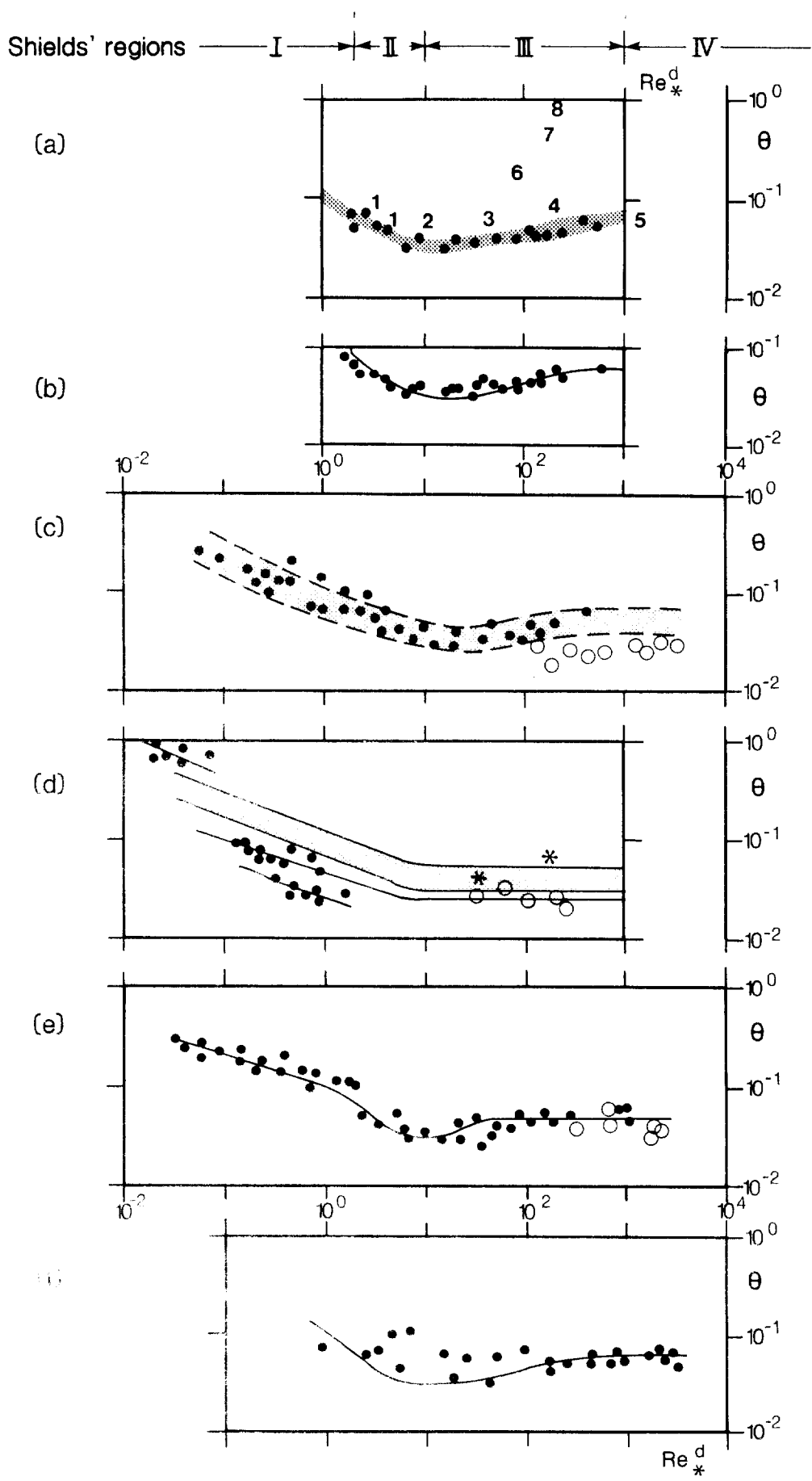


Fig 2:

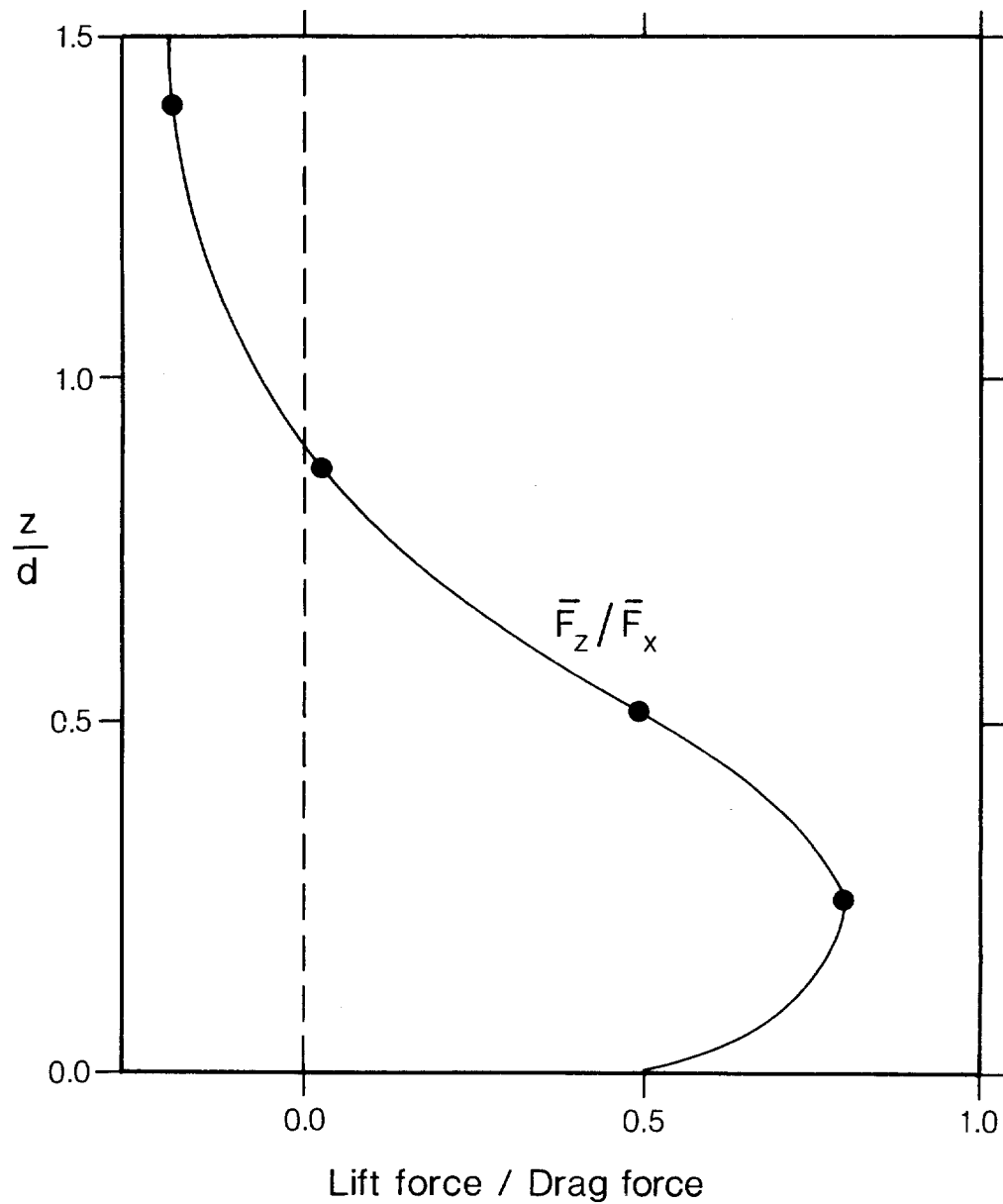


Fig 3: The ratio of mean lift force to mean drag force on a sphere of diameter  $d$  at height  $z$  measured from the top of a rough but level bed (after Apperley, 1968).

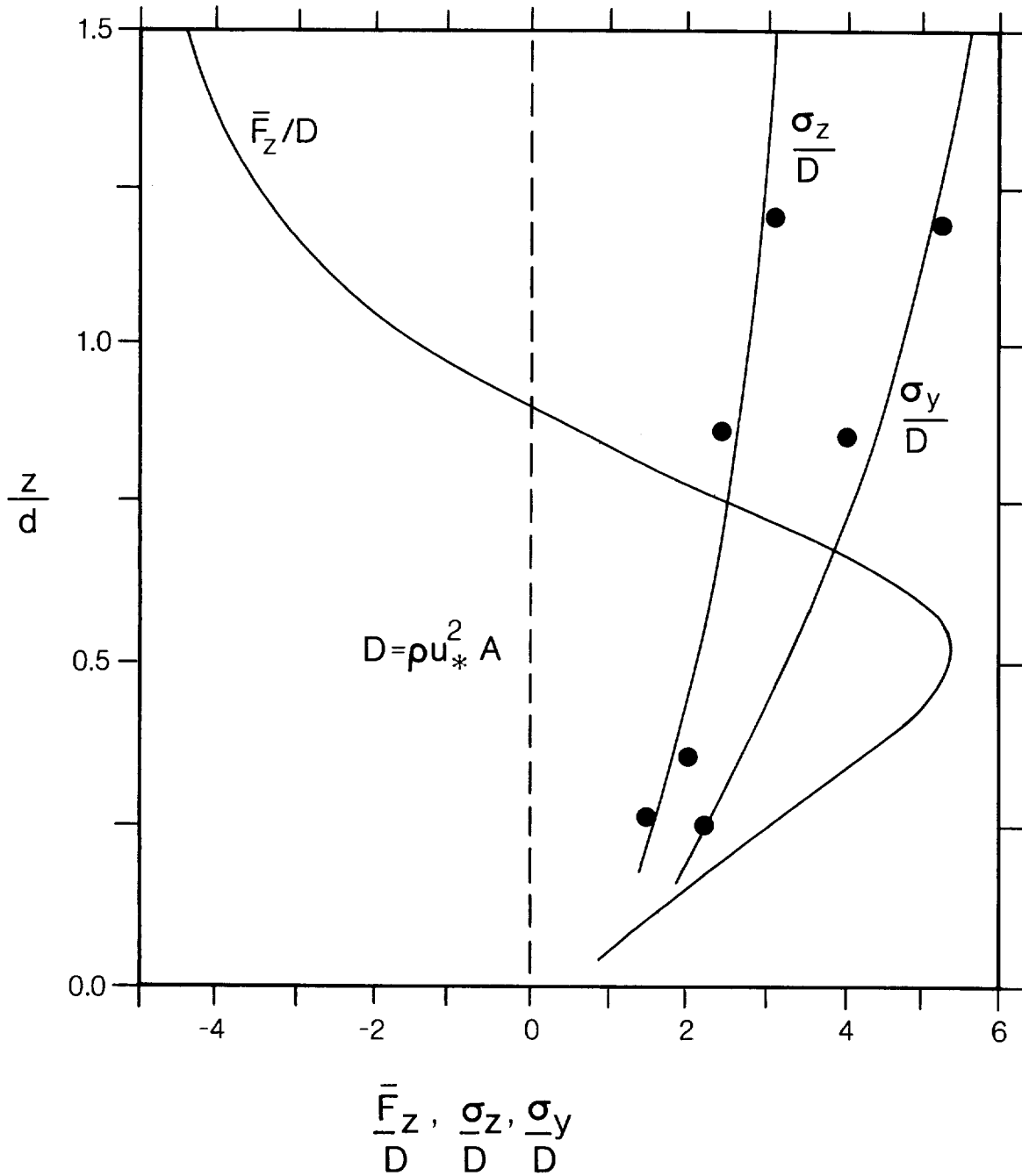


Fig 4: The mean lift force  $\bar{F}_z$  and root-mean-square ( $\sigma$ ) values of the lift component (z) and lateral component (y) on a sphere of diameter  $d$  for various heights  $z$  above the general level of the bed as a ratio of bed surface mean drag force  $\rho u_*^2 A$  (after Apperley, 1968).

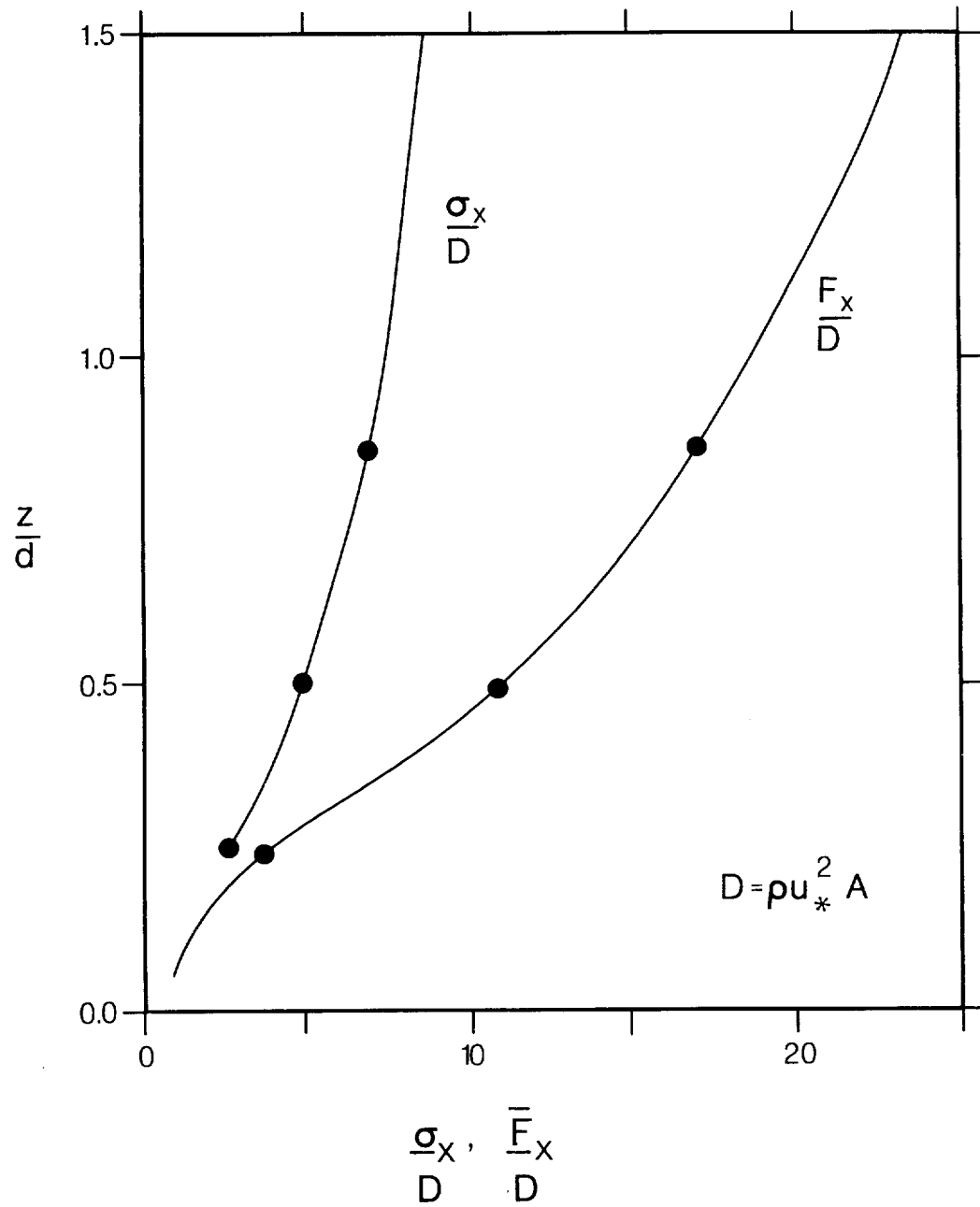
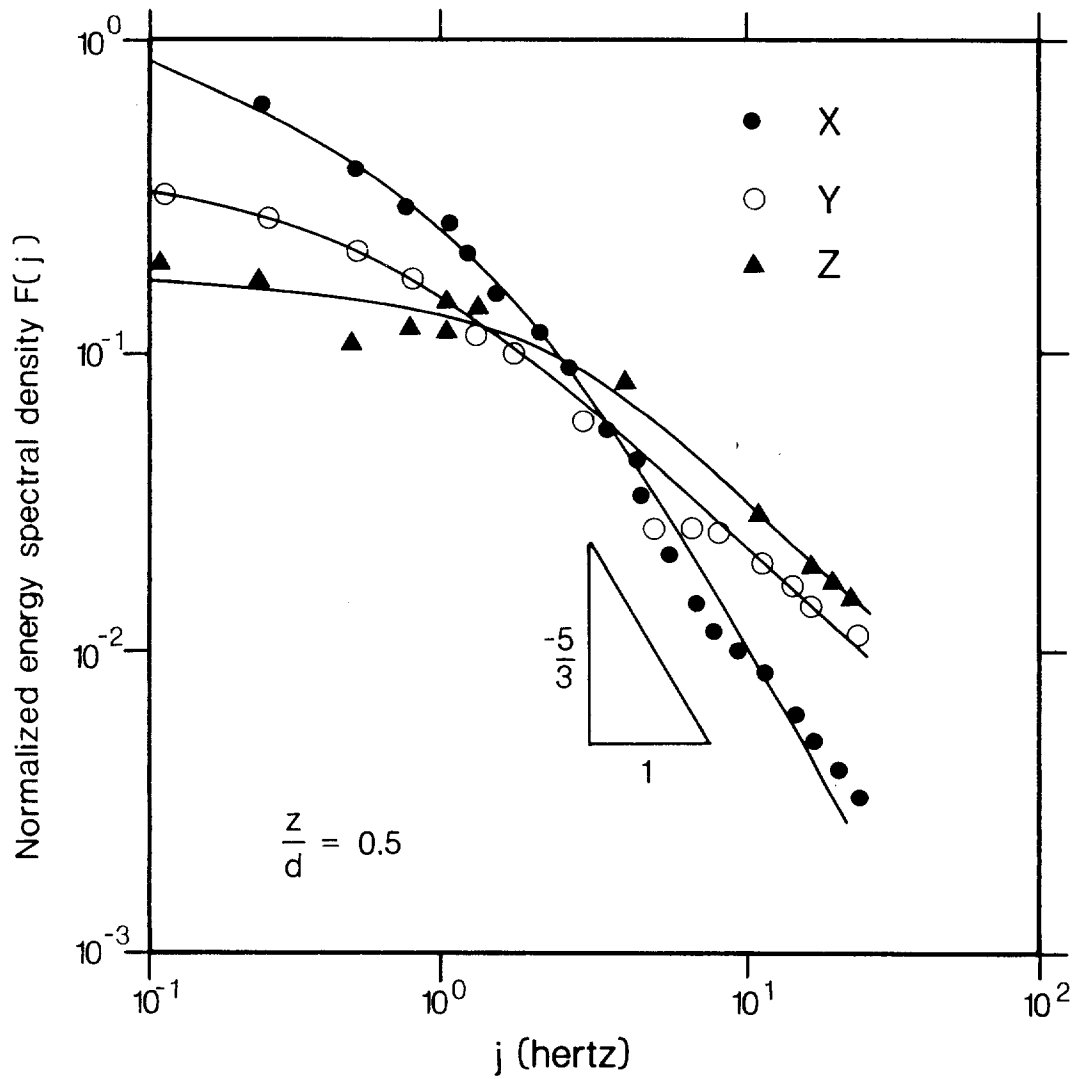


Fig 5: The mean ( $\bar{F}_x$ ) and root-mean-square ( $\sigma_x$ ) drag force as a ratio of bed surface mean drag force ( $\rho u_*^2 A$ ) on a sphere of diameter  $d$  for various heights  $z$  above the general level of the bed (after Apperley, 1968).



ig 6: Normalised energy spectral density of the measured turbulence force for each resolved component on a sphere at a height above the bed equal to the radius (after Apperley, 1968).

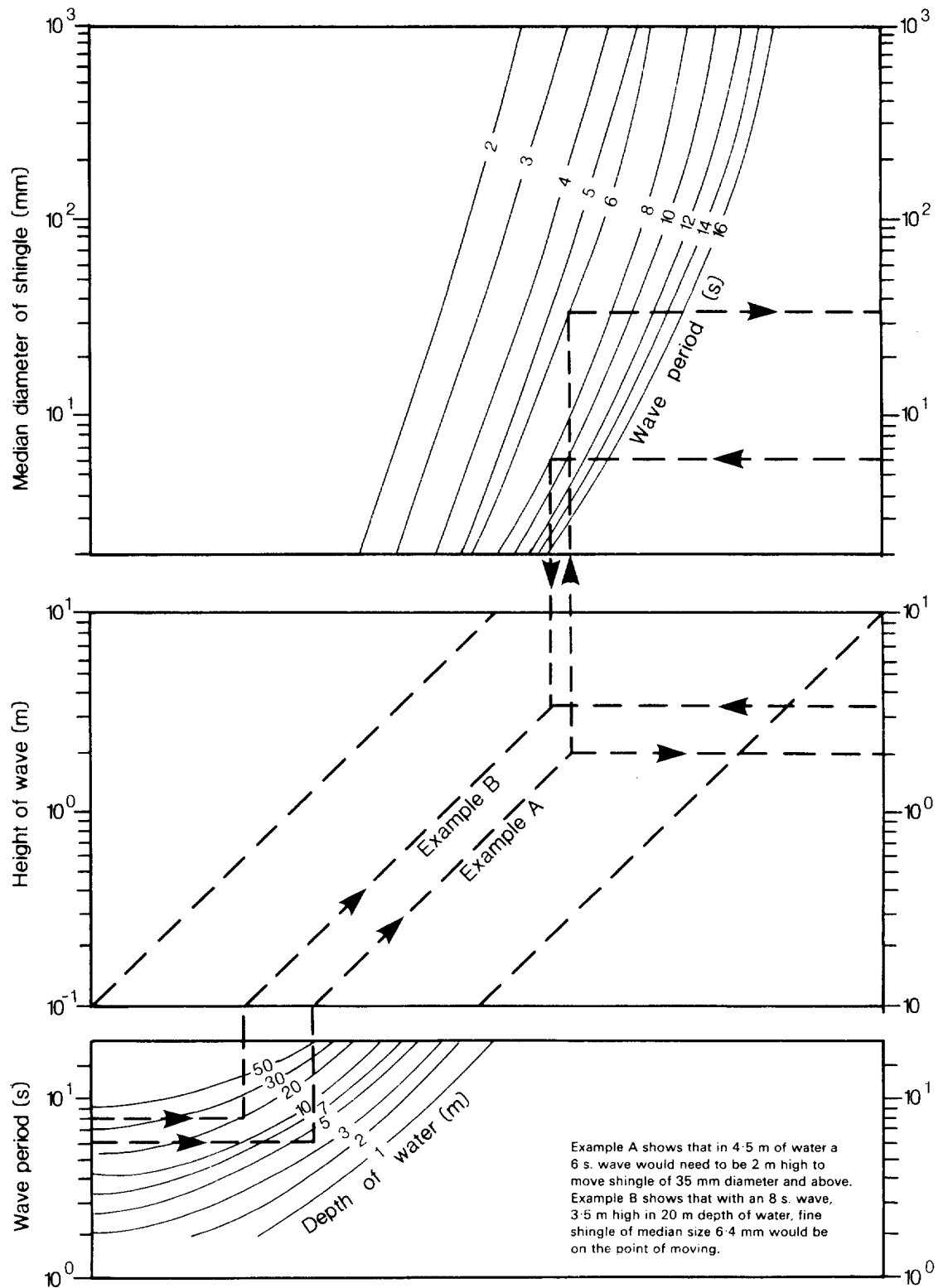


Fig 7: A working diagram giving threshold movement of shingle and gravel subj to wave action (after HRS note 15, Dec 1969).

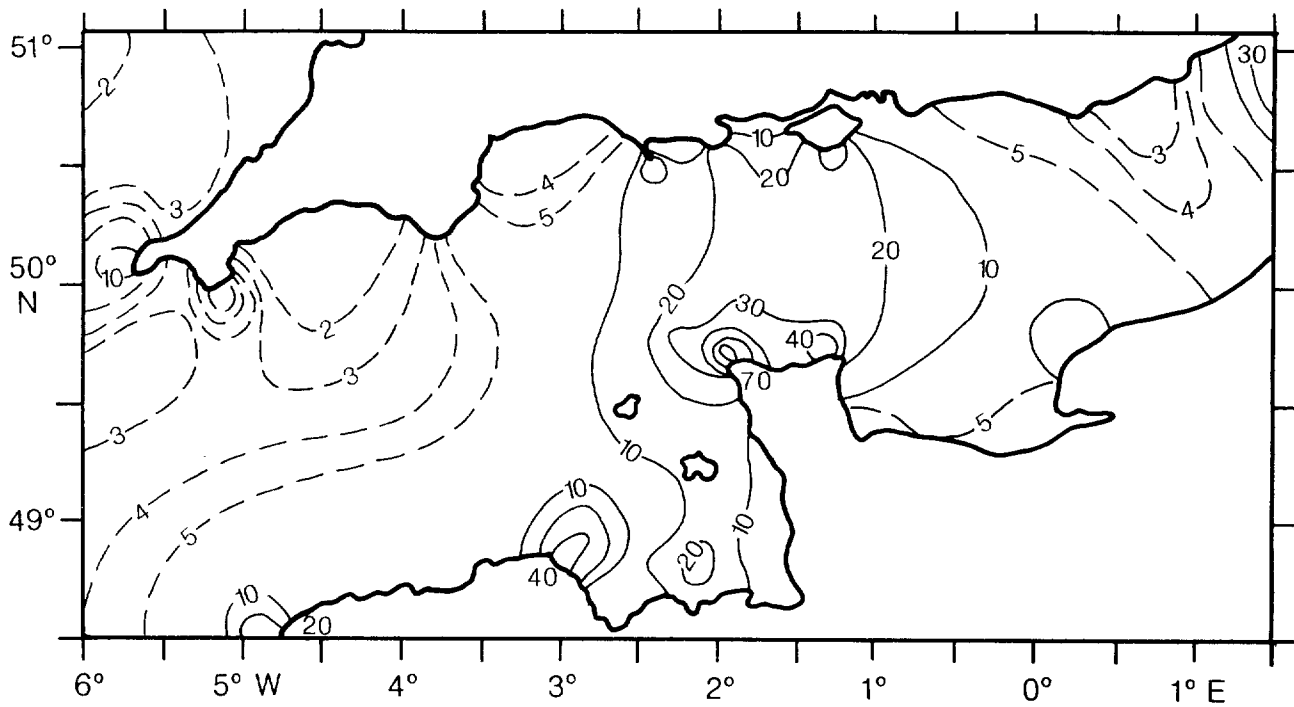


Fig 8: The mean value of the magnitude of the bottom shear stress (dynes/cm<sup>2</sup>) in the English Channel based on a numerical simulation (after Pingree, 1980).

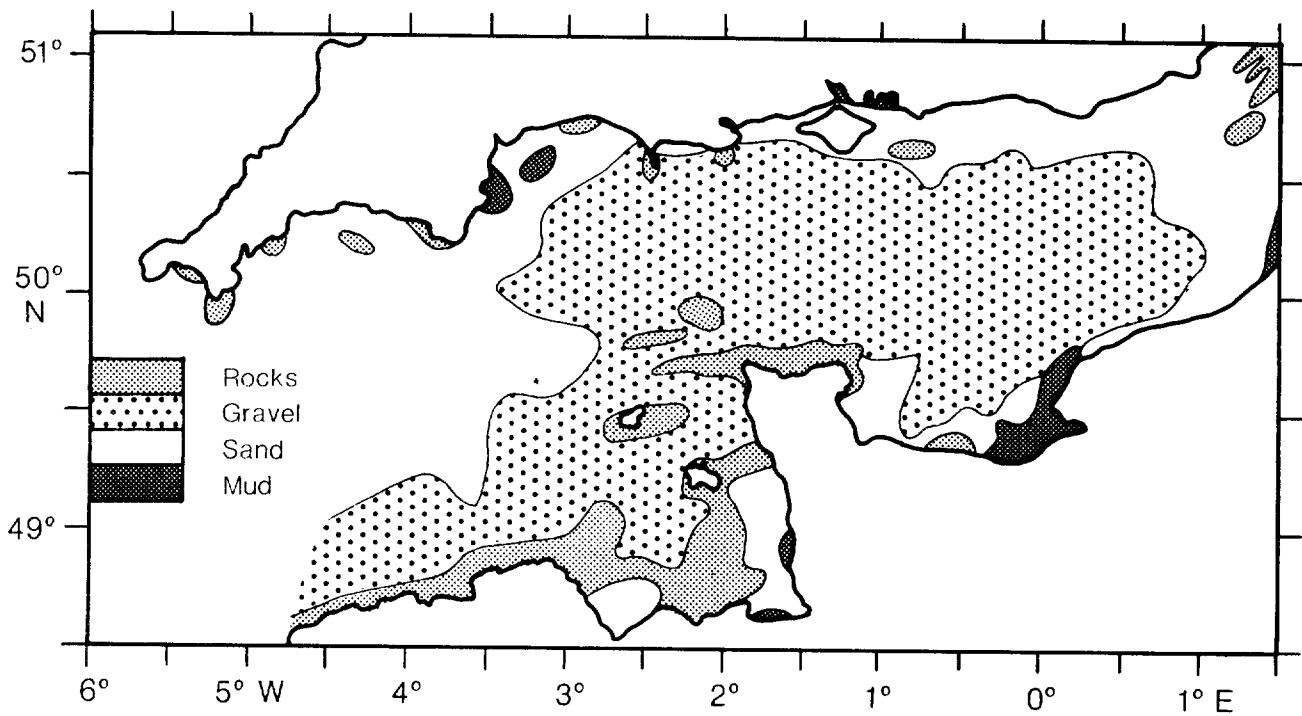


Fig 9: Nature of the bed in the English Channel showing bedrock in regions of stronger bottom shear stress (Fig 6) and sand and mud in regions of weaker bottom shear stress. Evidently, compared with Table 1 the figure is only intended to be a very general description of the bed particle size distribution (after Pingree, 1980).